1

Introduction to Detrital Apatite and Zircon Fission-track Thermochronology

Matthias BERNET
Institut des Sciences de la Terre, University Grenoble Alpes, France

Italienische Reise

Noch wunderlicher erschien ich diesem Begleiter, als ich auf allen seichten Stellen, deren der Fluß gar viele trocken läßt, nach Steinchen suchte und die verschiedenen Arten derselben mit mir forttrug. Ich konnte ihm abermals nicht erklären, daß man sich von einer gebirgigen Gegend nicht schneller einen Begriff machen kann, als wenn man die Gesteinsarten untersucht, die in den Bächen herabgeschoben werden, und daß hier auch die Aufgabe sei, durch Trümmer sich eine Vorstellung von jenen ewig klassischen Höhen des Erdaltertums zu verschaffen. Auch war meine Ausbeute aus diesem Flusse reich genug, ich brachte beinahe vierzig Stücke zusammen, welche sich freilich in wenige Rubriken unterordnen ließen.

Johann Wolfgang von Goethe, Palermo, 4 April 1787

1.1. Introduction

The use of detrital apatite and zircon fission-track and (U-Th)/He dating or white mica ^{40}Ar-^{39}Ar dating of modern river and beach sediments or

Fission-track Thermochronology,
coordinated by Marc JOLIVET.

ancient sandstone is a common approach in sediment provenance, source rock exhumation and basin analysis studies. In this chapter, the focus is on detrital apatite and zircon fission-track dating. Both techniques are considered as low-temperature thermochronology dating techniques, with temperature sensitivities in the range of ~ 250–180°C for zircon and ~ 130–80°C for apatite in comparison to high-temperature dating techniques such as zircon or monazite U-Pb dating (Figure 1.1).

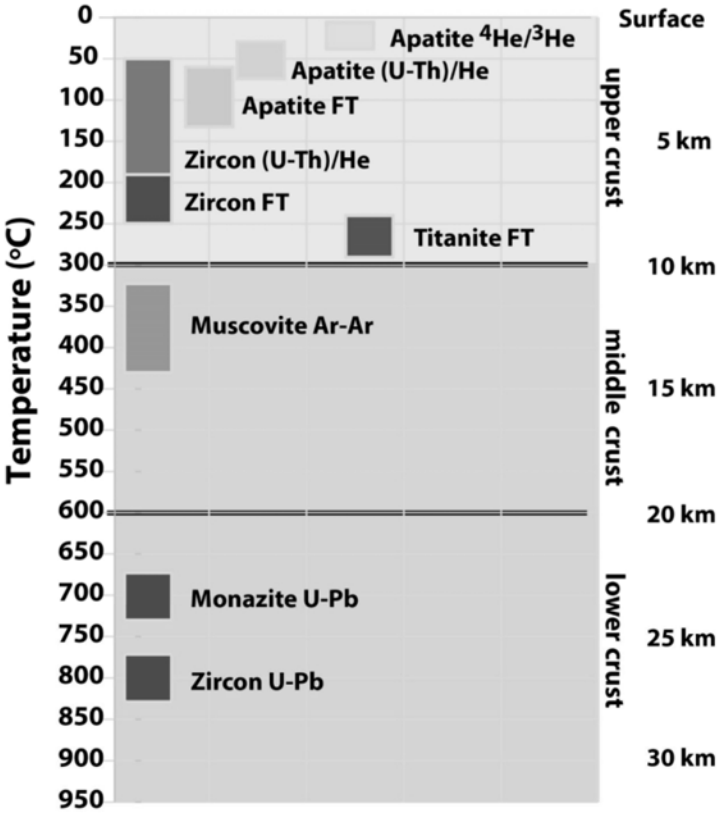

Figure 1.1. *Overview of the temperature sensitivity range of selected isotopic dating techniques. For a color version of this figure, see www.iste.co.uk/jolivet/fission.zip*

Apatite (density of 3.1–3.3 g/cm^3) and zircon (density of 4.5–4.6 g/cm^3) are heavy minerals in contrast to the density of quartz (2.65 g/cm^3). Despite the highly variable apatite and zircon fertility of many upper crustal plutonic, volcanic and metamorphic rocks, both apatite and zircon are relatively common accessory minerals in many sand-sized clastic sediments and sedimentary rocks (Malusà and Garzanti 2019). Although apatite is susceptible to dissolution in acid depositional environments (e.g. bogs) or soils, and abrasion during fluvial transport, zircon is considered as ultra-stable, as long as the grains have not accumulated too much α-radiation damage and are metamict (Malusà and Garzanti 2019; Malusà and Fitzgerald 2020). Both minerals are chemically stable under diagenetic conditions during burial in sedimentary basins or during basin inversion and exhumation.

Since the first detrital zircon fission-track analysis studies in the 1980s (e.g. Hurford et al. 1984; Cerveny et al. 1988), detrital apatite and zircon fission-track dating have developed into standard techniques that have been applied successfully to many different geodynamic settings, for example, the European Alps, the Himalaya, the Tibetan plateau, the Andes, the Southern Alps of New Zealand, or in Alaska, for quantifying exhumation or erosion rates, determining the timing of tectonic events, or the thermal history of sedimentary basins (see examples and references below). Today, it is possible to combine fission-track dating with U-Pb dating and even with (U-Th)/He dating for double and triple dating of single grains, as well as chemical analyses such as Sr isotopes in apatites and Lu and Hf isotopes in zircon. The combination of different techniques on single grains may provide additional valuable information for constraining more precisely sediment provenance and source rock or basin thermal histories.

This chapter provides an introduction to (A) the basics of detrital fission-track analysis using the external detector method (EDM), (B) the underlying statistics for age calculations, data interpretation and the evaluation of detrital grain age distributions, and (C) applications of detrital thermochronology with some examples.

1.2. Principals of fission-track dating

1.2.1. *Basics of single grain apatite and zircon fission-track analysis*

Fission-track dating has been developed in the 1960s by Robert L. Fleischer, P. Burford Price and Robert M. Walker, three physicists of General Electrics in Schenectady, New York, USA, who worked on nuclear defects in solids. The formation of a fission track by spontaneous fission of ^{238}U isotopes is in fact a very rare event as radioactive ^{238}U isotopes normally decay by a series of α and β-decay steps to stable ^{206}Pb (Figure 1.2(A)). The regular ^{238}U to ^{206}Pb decay is about 2 million times more common than the spontaneous fission decay of ^{238}U into two isotopes of different mass that recoil from each other and leave a damage zone in the crystal structure, which is called a latent track (Table 1.1; Figure 1.2(B)) (Fleischer et al. 1975; Wagner and Van den haute 1992). Early on Fleischer, Price and Walker realized that the formation of latent damage zones by spontaneous fission of ^{238}U isotopes in crystals of U-bearing minerals such as apatite, zircon or titanite could be of geological interest (e.g. Price and Walker 1962; Fleischer and Price 1964; Fleischer et al. 1975). The isotopes formed during the spontaneous fission events are not always the same. In fact, two of over 690 different possible isotopes, one heavier isotope with a mass number of up to 172 and a lighter isotope with a mass number as low as 66, are formed. Most of these newly formed isotopes are also radioactive and will decay over seconds, hours, days, months or years, but without causing additional fission damage. The formation of spontaneous fission-track damage in a U-bearing crystal follows a decay constant, just like regular α-decay, and the fission tracks that are formed because of the spontaneous fission decay of ^{238}U are regarded as the daughter products of this decay event (Table 1.1). Given the isotopic abundance and the spontaneous fission-decay constant of ^{238}U isotopes with respect to ^{235}U, ^{234}U and ^{232}Th, only ^{238}U is considered as important for fission-track dating, and the contributions of spontaneous fission tracks from ^{235}U, ^{234}U and ^{232}Th spontaneous fission are negligible. In dependence of U content, fission tracks accumulate in crystals over time and will be at least partially preserved, if the ambient temperatures are below the so-called closure temperature (*Tc*).

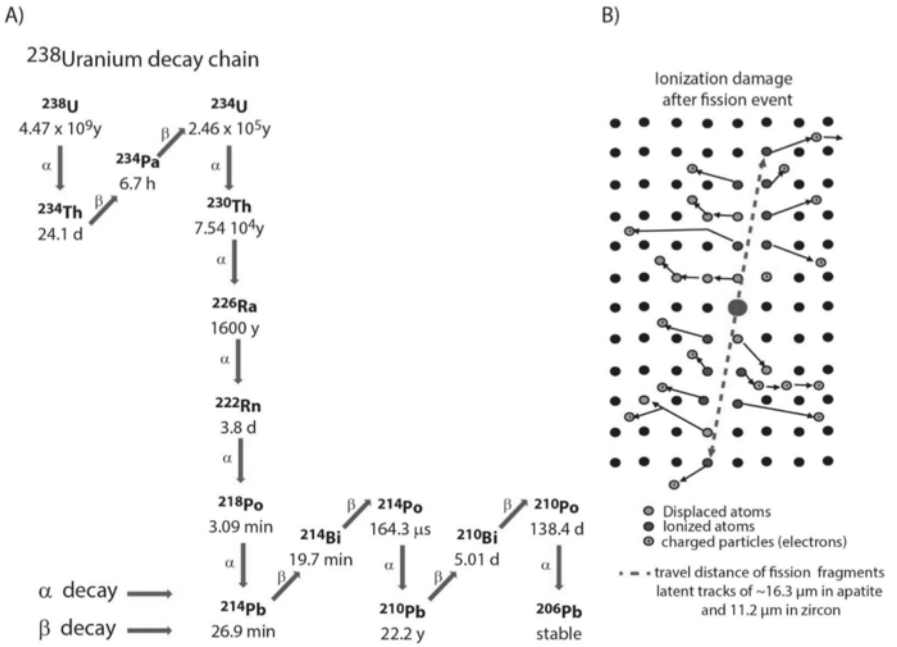

Figure 1.2. *(A) ^{238}U-^{206}Pb decay chain, with a series of eight α-decay steps and six β-decay steps and their half-lives. (B) Spontaneous fission of ^{238}U and formation of latent fission tracks. For a color version of this figure, see www.iste.co.uk/jolivet/fission.zip*

Isotope	Abundance (%)	Decay Constant (year^{-1})	Half-life (year)	Thermal neutron capture cross-section (10^{-24} cm^2)
^{238}U	99.2743	(α) 1.55×10^{-10} (s.f.) $\sim 7.5 \times 10^{-17}$	(α) 4.47×10^{9} (s.f.) $\sim 1.3 \times 10^{16}$	2.7
^{235}U	0.7200	9.85×10^{-10}	7.04×10^{8}	580
^{234}U	0.0057	2.81×10^{-6}	2.46×10^{5}	100
^{232}Th	100.0000	4.92×10^{-11}	1.41×10^{10}	7.4

Table 1.1. *Decay constants and half-lives of U and Th isotopes. Note: α for α-decay, s.f. for spontaneous fission decay (from Wagner and Van den haute (1992); Donelick et al. (2005))*

1.2.2. *Closure temperature concept*

The *Tc* is the temperature at which an isotopic system closes to the loss of daughter products (Dodson 1973). In case of fission-track dating, it means that fission tracks are preserved and not lost to total annealing, which occurs at elevated temperatures above the closure temperature. The *Tc* of the apatite and zircon fission-track dating systems, and also other thermochronological systems such as (U-Th)/He or $^{40}Ar/^{39}Ar$ dating, depends primarily on cooling rate (Figure 1.3(A)). Equation [1.1] shows that the *Tc* is controlled by diffusion and can be calculated as follows:

$$T_c = \frac{E_a}{R\ln\left(A\tau\frac{D_0}{a^2}\right)} \qquad [1.1]$$

where *Ea* is the activation energy, *R* is the gas constant, *A* is the cylinder shape of the crystal, τ is the characteristic time taken for the diffusivity to decrease by a factor *e* and Do/a^2 is the diffusion. Because the calculation of τ also requires a *Tc* value (see equation [1.2]), it is necessary to find an iterative solution for *Tc*. Table 1.2 shows commonly used values of activation energy and diffusion parameters for apatite and zircon fission-track dating determined by laboratory diffusion experiments (see summary in Wagner and Van den haute (1992); Reiners and Brandon (2006)).

$$\tau = -\frac{RT_c^{\,2}}{E_a\frac{\partial T}{\partial t}} \qquad [1.2]$$

Equation [1.2] also shows why the cooling rate, the change of temperature (δT) over time (δt), has an important influence on the *Tc*. The parameter τ is linked to diffusion, as that annealing of fission tracks, which will be discussed in more detail below, is controlled by the diffusion of atoms and electrons that were displaced in the crystal structure during the spontaneous fission event, back into place to repair or anneal the damaged area (latent track) of the crystal. The diffusion ($D_{(t)}$) equation is shown in equation [1.3]:

$$D_{(t)} = D_{(0)}e^{-t/\tau} \qquad [1.3]$$

where $D_{(0)}$ is the diffusivity constant, *t* is the time and τ is again the characteristic time given in equation [1.2]. The graphic in Figure 1.3(B) relates

the number of spontaneous tracks Ns counted on an internal crystal surface today to the time when the crystal apparently cooled below the effective *Tc* and the fission-track dating system changed from an open system, where fission track was rapidly lost to annealing, to a closed system, where all newly formed fission tracks were preserved in the crystal at lower temperatures (Braun et al. 2006). We must keep in mind that the *Tc* concept should only be applied for interpreting the thermochronological data of rocks that experienced relatively rapid (≥ 10–15°C/Myr) monotonic cooling. For detrital grains collected from modern or ancient clastic sediments, this assumption may only be justified for the youngest grain age populations (see below). Furthermore, for apatite crystals, the chemical composition of the apatites has an influence on the *Tc* and the annealing of fission tracks, as F-apatites tend to have a lower *Tc* than Cl-apatites (Figure 1.3(B)) (Donelick et al. 2005; Reiners and Brandon 2006). For zircons, it is rather the amount of accumulated α-radiation damage from regular ^{238}U, ^{235}U and ^{232}Th α-decay (α-recoil damage) that will have an influence on the *Tc*. It is important to distinguish between zero-damage zircons and α-radiation damaged zircons. Zero-damage zircons have not accumulated significant amounts of α-radiation damage before cooling below the zircon fission-track *Tc*. Such zircons must cool very rapidly from crystallization or high-grade metamorphic temperatures below the zircon fission-track *Tc* (Rahn et al. 2004; Reiners and Brandon 2006). With certain exceptions of modern river sediments derived from zones of active volcanism, or rapidly exhuming orogenic mountain belts such as in the Himalayan syntaxes, Taiwan, or the Southern Alps of New Zealand, most detrital zircons will be considered as α-radiation damaged, as only a few million years and average U concentrations are needed to damage the crystals enough to no longer be considered as zero-damage grains. α-Radiation-damaged zircons tend to have *Tc*s about 100°C lower than zero-damage zircons (Figure 1.3(A)). We can see that the zircons have accumulated α-radiation damage through their change in color from clear transparent crystals when they have no or very little radiation damage, to yellow, pink or violet-red colors when there is an increasing amount of α-radiation damage. Similar to fission tracks, α-radiation damage can be annealed, but at higher temperatures than fission tracks (Garver and Kamp 2002). Using Raman spectroscopy, it is possible to determine the impact of α-radiation damage on the crystal structure of zircons (e.g. Guenthner et al. 2013, 2017).

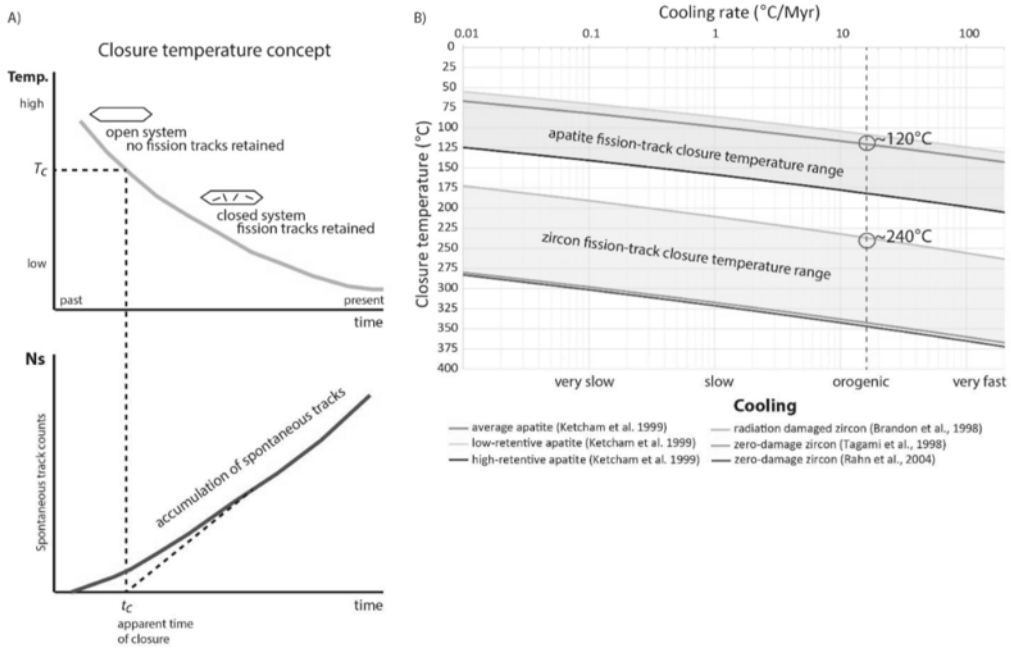

Figure 1.3. *(A) Closure temperature concept (modified after Braun et al. 2006). (B) Dependence of closure temperature on cooling rate. Data taken from the Closure program of Brandon (see Ehlers et al. (2005)). Apatite of average chemical composition, low-retentive F-apatite (Renfrew) and high retentive Cl-apatite (Tioga), all from Ketcham et al. (1999). Radiation damaged zircon from Brandon et al. (1998), and zero-damage zircon from the fanning models by Rahn et al. (2004) and Tagami et al. (1998). Orogenic cooling refers to commonly observed cooling rates in orogens such as the European Alps. The red stippled line indicates in the literature commonly cited closure temperatures of 120°C for apatite of average chemical composition and 240°C for natural radiation damaged zircon. For a color version of this figure, see www.iste.co.uk/jolivet/fission.zip*

Parameter	AFT Tc	AFT 90%	AFT 10%	AFT (L) Tc	AFT (L) 90%	AFT (L) 10%	AFT (H) TC	AFT (H) 90%	AFT (H) 10%
E_a (kj mol^{-1})	147.2	127.4	160.7	138.2	124.4	149.9	186.7	139.8	231.8
Omega (= 55 Do/a_s^2) (s^{-1})	2.05E+6	2.67E+5	1.55E+7	5.08E+5	1.91E+5	4.39E+6	1.57E+8	1.41E+6	3.38E+10
	ZFT Tc	ZFT 90%	ZFT 10%	ZFT[1] (0) Tc	ZFT[1] (0) 90%	ZFT[1] (0) 10%	ZFT[2] (0) TC	ZFT[2] (0) 90%	ZFT[2] (0) 10%
E_a (kj mol^{-1})	221.0	225.0	221.0	321.0	272.0	339.0	324.0	231.0	359.0
Omega (= 55 Do/a_s^2) (s^{-1})	1.24E+8	2.62E+11	1.24E+8	5.66E+13	5.66E+13	5.66E+13	1.64E+14	1.09E+12	1.02E+15

Table 1.2. *Activation energies and diffusion parameters for apatite and zircon fission-track dating. Note: AFT = apatite fission track (average composition, Ketcham et al. 1999); AFT (L) = low retentivity (F-apatite, Ketcham et al. 1999); AFT (H) = high retentivity (Cl-apatite, Ketcham et al. 1999); ZFT = zircon fission track (natural α-radiation damaged, Brandon et al. 1998); 1 zero damage fanning model (Rahn et al. 2004); 2 zero damage fanning model (Tagami et al. 1998). 90% (retention) = upper PAZ limit; 10% (retention) = lower PAZ limit. Data taken from the Closure Program of Brandon (see Ehlers et al. (2005))*

1.2.3. *Partial annealing zone concept*

In many geological settings, rocks will not have simple, relatively fast and monotonic cooling histories, but rather complex thermal histories with variable cooling rates and/or episodes of reheating. That fission tracks are susceptible to shortening and track annealing was recognized early on by Wagner (1969). Slow cooling or reheating to elevated temperatures may cause partial annealing of fission tracks in apatite and zircon over a certain temperature range, which is defined as the partial annealing zone (PAZ). Particularly when dealing with detrital apatites and zircons obtained from ancient sandstone from drill cores or from outcrops of inverted basins, the impact of post-depositional burial heating needs to be taken into account (e.g. Briggs et al. 1981; Naeser 1981). During reheating, partial annealing of fission tracks will only occur as long as the ambient temperature during reheating is not surpassing the *Tc* of the thermochronometer.

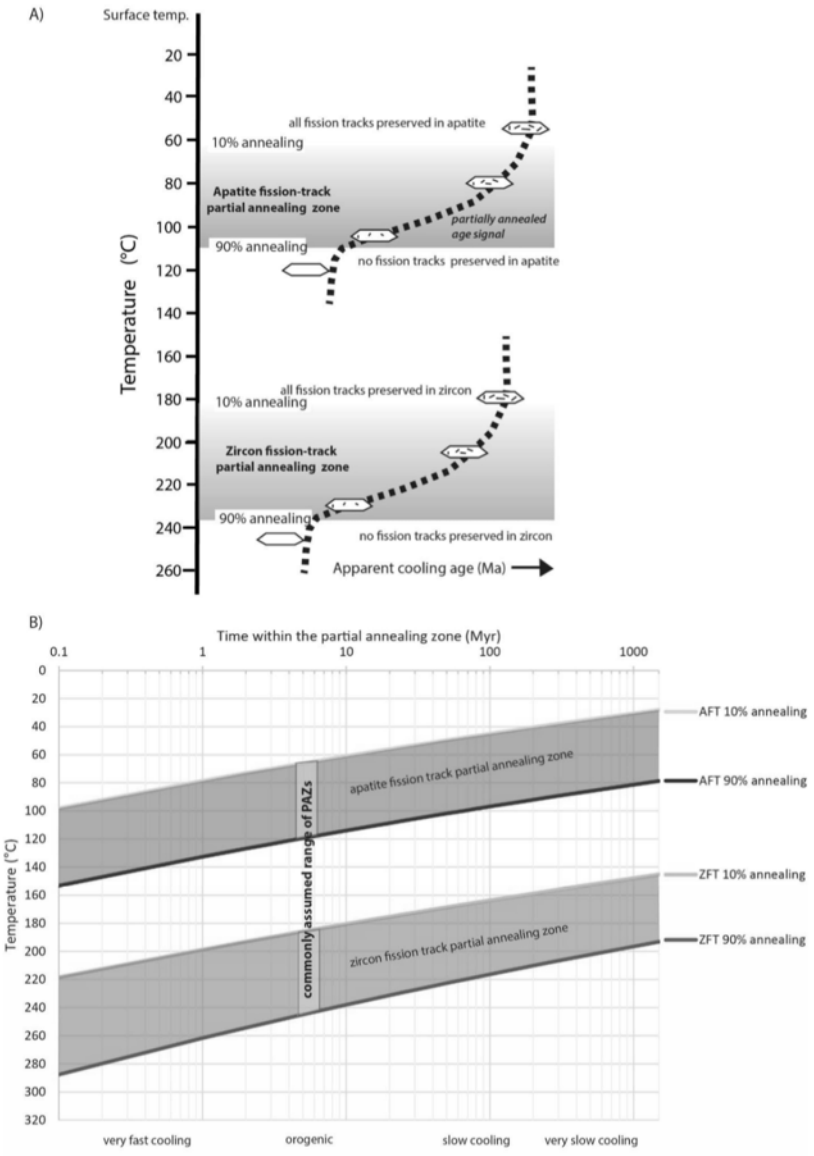

Figure 1.4. *(A) Partial annealing zone concept of decreasing apparent fission-track age with increasing temperature through the partial annealing zone (PAZ). (B) Dependence of the partial annealing zone temperature range on residence time for apatites of average chemical composition and radiation damaged zircons (data taken from the Closure program of Brandon (see Ehlers et al. (2005)). For a color version of this figure, see www.iste.co.uk/jolivet/fission.zip*

This does not mean that the *Tc* defines the lower limit of the PAZ. The lower limit of the PAZ is rather defined as the temperature at which 90% of the fission tracks are affected by annealing, whereas the upper limit of the PAZ is the temperature at which 10% of the fission tracks are affected by annealing (e.g. Reiners and Brandon 2006). The progressive shortening of the mean track lengths results in younger apparent fission-track ages in sedimentary rocks with depth in a sedimentary basin, in dependence of burial heating and the (paleo-)geothermal gradient. Figure 1.4 shows the dependence of the apatite and zircon fission-track PAZ for apatites of average chemical composition and for α-radiation damaged zircons, as well as the hold time in millions of years within the PAZ.

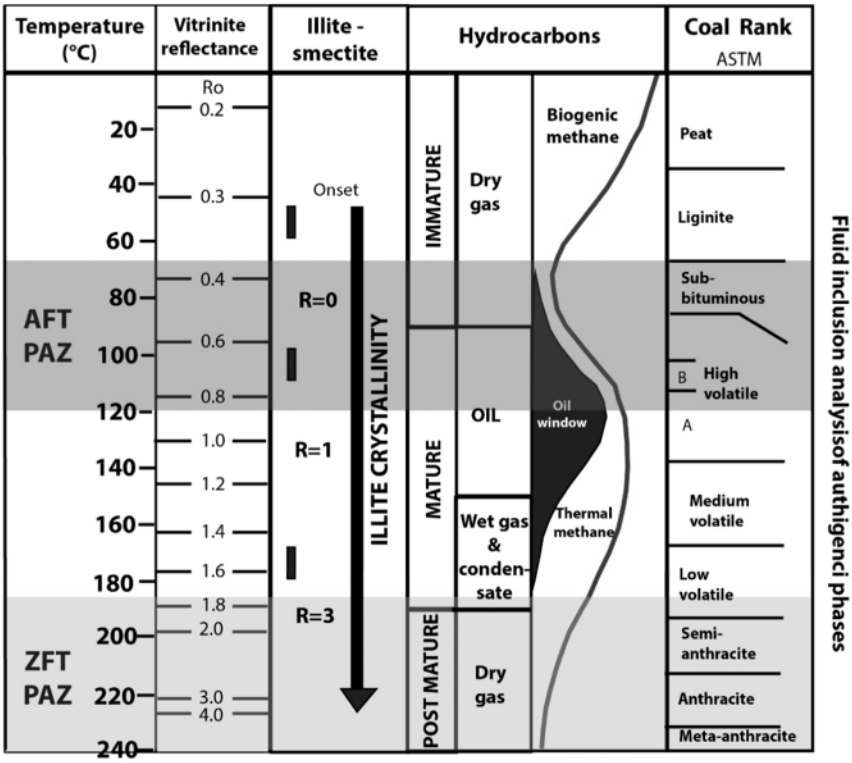

Figure 1.5. *Comparison of the partial annealing zone temperature ranges for fission tracks of apatites of average chemical composition and radiation damaged zircon with vitrinite reflectance, illite-smectite mixed-layer ordering, hydrocarbon production and coal rank. For a color version of this figure, see www.iste.co.uk/jolivet/fission.zip*

In combining the apatite fission-track lengths measurements with independent thermal information from borehole temperature measurements (present-day geothermal gradient) and vitrinite reflectance measurements (paleo-geothermal gradient estimates), it was shown that in many basins, total annealing of fission tracks in apatite occurred at temperatures that correspond to vitrinite reflectance values of about Ro% 0.7 and the peak of oil generation within the oil window (Figure 1.5; Dow 1977; Briggs et al. 1981; Naeser 1981; O'Sullivan 1999; Armstrong 2005). For this reason, apatite fission-track dating and track lengths measurements became very popular with the oil industry and the kinetics of track annealing in apatite were studied in great detail (e.g. Green and Durani 1977; Green et al. 1986; Laslett et al. 1987; Carlson et al. 1999; Donelick et al. 1999; Barbarand et al. 2003; Ketcham et al. 2007).

The PAZ concept is equivalent to the partial retention zone (PRZ) concept for (U-Th)/He dating (e.g. Farley 2002; Reiners 2005; Guenthner et al. 2013; Gautheron and Brichau, this volume). For more comprehensive information on the *Tc* and the PAZ/PRZ for fission-track dating and other thermochronometers, please see the books and articles by Reiners and Ehlers et al. (2005), Braun et al. (2006), Guenthner et al., (2017), Ault et al. (2019), Malusà and Fitzgerald (2019), Gérard et al. (2022), or the summary by Reiners and Brandon (2006).

1.3. Sample preparation and fission-track dating

1.3.1. *Sample preparation*

In order to do fission-track dating of apatite and zircon, we must separate the apatite and zircon grains from rocks or sediments. In detrital thermochronology, this would mean to either separate the apatites and zircons from medium to coarse grained sandstones or from modern beach or river sediments. The sampling of modern sediments is very easy and samples can be preprocessed in the field by sieving and panning with gold wash pans for increasing the concentration of heavy minerals of the sample relative to the light fraction (Figure 1.6). No significant sampling bias with respect to the later observed fission grain age spectrum is introduced by panning and hydraulic sorting (Malusà and Garzanti 2019), but if we want to determine the heavy mineral spectrum of a modern river or beach sample quantitatively, sieving and panning in the field are not recommended, and bulk sediment samples need to be taken.

Figure 1.6. *Sampling of modern river sediments for detrital fission-track studies. (A) Selection of sampling site will in many cases depend on access. Gravel and/or sand bars along the river bank are preferable. If possible, heavy mineral placer deposits can be used. (B) Sieve sediment to eliminate very coarse sand and gravel. (C and D) Wash out all mud and reduce the light mineral fraction to concentrate heavy minerals, which is in many locations black (magnetite) and/or red (garnet). Apatites and zircons will be in this fraction. (E) Transfer sample material into bag and repeat the whole procedure 8–10 times to collect about 200 g of sample material. (F) Take note of all the lithologies in the drainage basin represented in the river gravels and boulders. Also record the sampling location with GPS coordinates and/or on a map. For a color version of this figure, see www.iste.co.uk/jolivet/fission.zip*

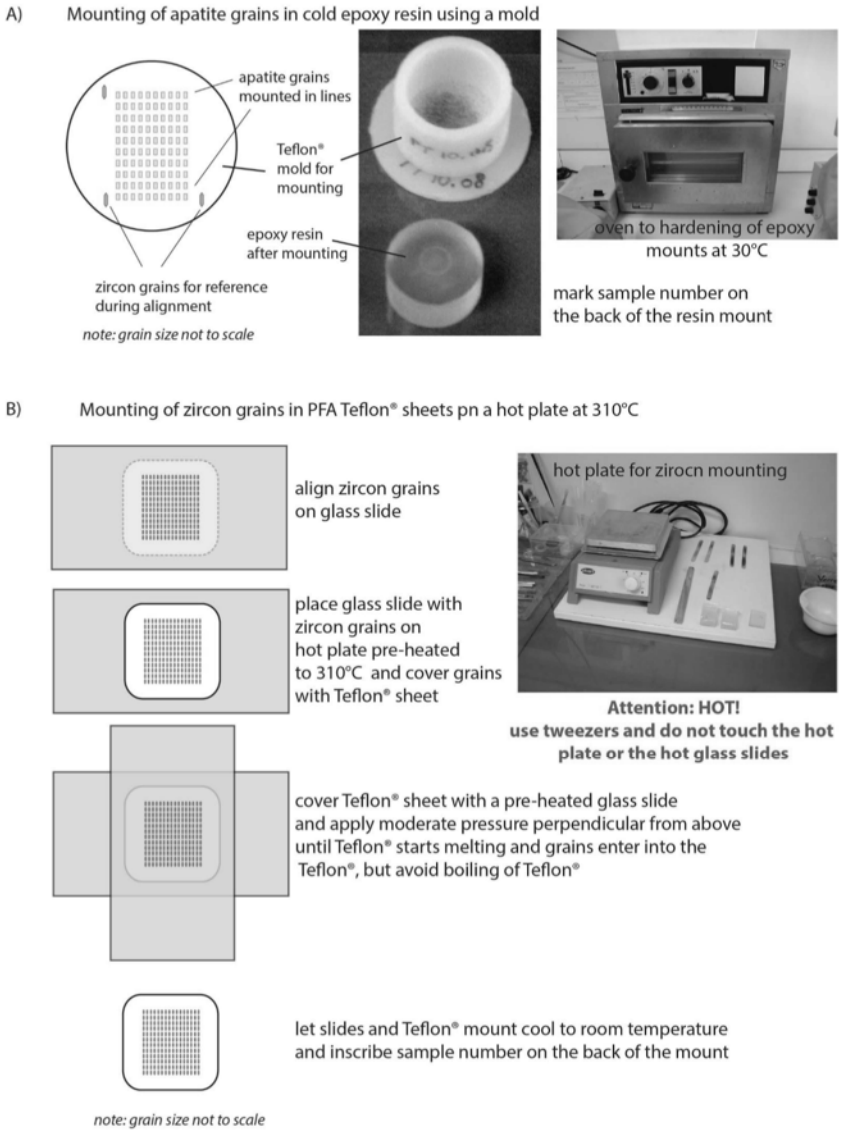

Figure 1.7. *Mounting for fission-track analysis of (A) apatite grains in cold resin and (B) zircon grains in PFA Teflon® sheets at 310°C on hot plate using a "sandwich" technique between two glass slides. For a color version of this figure, see www.iste.co.uk/jolivet/fission.zip*

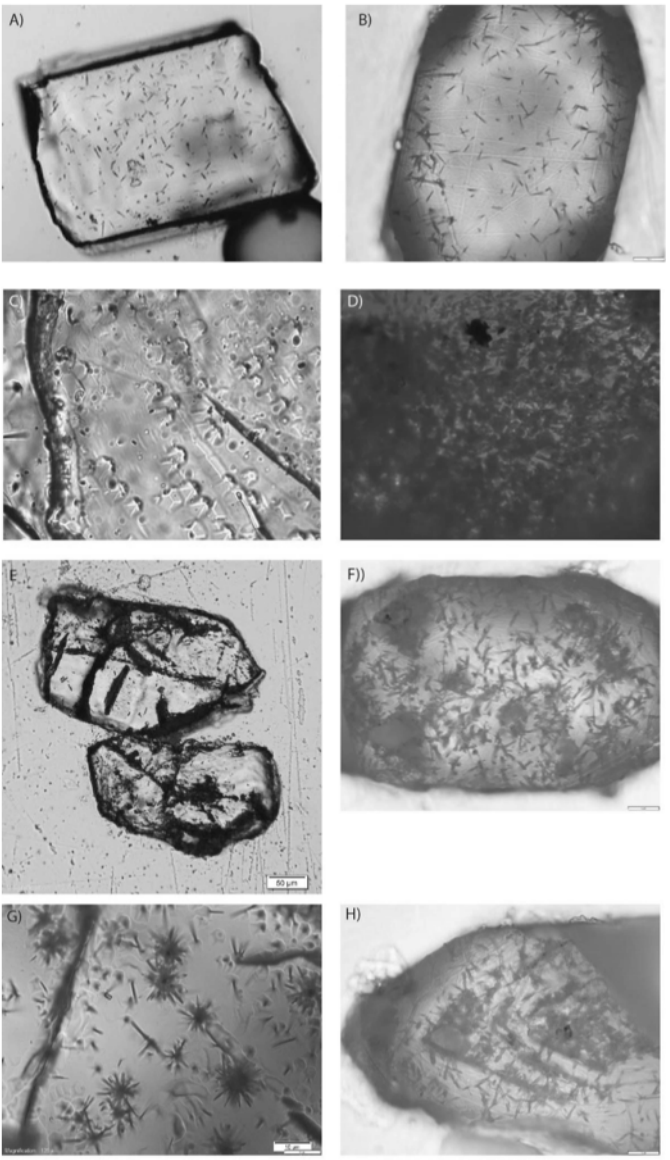

Figure 1.8. *Examples of well-etched (A) apatite and (B) zircon crystals mounted parallel to the c-axis. Examples of problematic grains: (C) etch pits in apatite grain not mounted parallel to the c-axis; (D) over-etched zircon with very high track density; (E) apatites with many crystal defects and fractures; (F) zircon with many inclusions and patchy U distribution; (G) apatite with zircon inclusions and not mounted parallel to c-axis; (H) zircon with strong U-zonation*

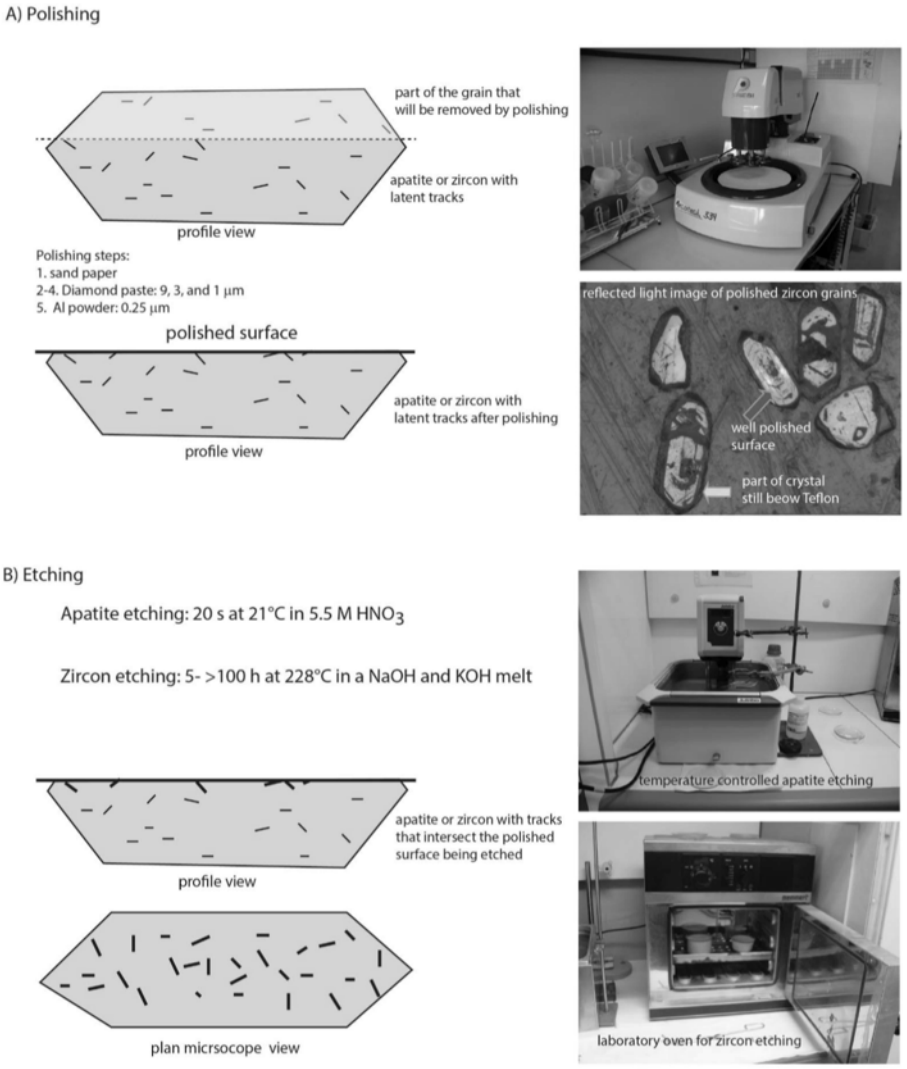

Figure 1.9. *(A) Grain mount polishing and (B) etching procedures for apatite and zircon fission-track analysis. For a color version of this figure, see www.iste.co.uk/jolivet/fission.zip*

Sandstone samples cannot be preprocessed in the field. In most laboratories, 7–10 kg of each sandstone sample collected in the field have to be crushed in a jaw-crusher and disc-pulverizer to disintegrate the rocks and liberate the grains.

After sieving the sample to separate the 200–80 μm fraction, many labs will pass the samples over a hydraulic shaking table (Gemini or Wilfley tables) to concentrate the heavy mineral fraction. Of course, these sample preparation steps will not be needed for the modern sediment samples that are preprocessed in the field. All samples will be dried at low temperatures of ~ 30–40°C in a laboratory oven before magnetic and heavy liquid separations. Magnetic separation serves for removing all minerals that have magnetic properties (e.g. magnetite, hematite, biotite and amphibole) from the nonmagnetic minerals such as apatite and zircon. Heavy liquid separation with tetrabromomethane (caution: toxic substance!) or the nontoxic sodium polytungstate, with densities of about 2.9 g/cm^3, allows us to separate the heavy minerals from the remaining light mineral fraction of quartz and feldspar. A second heavy liquid separation step with methylene iodide (density of 3.3 g/cm^3) allows the separation of the so-called apatite fraction from the zircon fraction. Nevertheless, these two fractions may still contain other heavy minerals, particularly pyrite and kyanite in the zircon fraction, which may require picking apatites and zircons by hand. For more information on heavy mineral separation procedures, see Kohn et al. (2019).

Once the apatite and zircon aliquots were obtained, we can start mounting the grains for fission-track analysis. Apatite crystals are mounted in an epoxy resin and zircon crystals are mounted in Teflon sheets (Figure 1.7). It is recommended to align the grains during mounting, particularly in case double or triple dating in combination with U-Pb and (U-Th)/He dating of singles is planned. For a bedrock sample, between 20 and 25 grains are commonly dated per sample and for detrital samples, as many grains as possible up to 100–120 grains per sample (e.g. Vermeesch 2004). Not all mounted grains are suitable for fission-track dating because of crystal defects, inclusions, strong U-zoning, grains not mounted parallel to the c-axis, and particularly for zircon: under- or over-etched tracks (Figure 1.8), it is recommended to mount at least 200–300 grains per mount for bedrock samples and up to 500 grains per mount for detrital samples.

The etching procedure to reveal spontaneous fission tracks in apatite is very simple and commonly only one mount is prepared per sample. For detrital zircons, a multi-mount approach is recommended to reveal countable fission tracks across the whole grain age spectrum (e.g. Naeser et al. 1987; Bernet et al. 2004a).

After mounting, the grain mounts are polished, using several polishing steps (e.g. sand paper, 9 μm, 3 μm and 1 μm diamond paste, and 0.25 μm Al powder) to remove part of the crystal and to expose a well-polished internal surface (Figure 1.9). The quality of the polishing needs to be carefully controlled with a reflected light microscope to see that the grains are well exposed and the surfaces are smooth. The grain mounts are then ready for etching. The recommend etching procedure for apatites is with 5.5 M HNO_3 at 21°C for 20 s (Donelick et al. 2005; Kohn et al. 2019). The etching procedure for zircon is more complex. Zircons will in many labs be etched in a NaOH and KOH melt at 225–230°C in a laboratory oven for as few as 3–4 h and up to > 100 h. If the etch time selected is too short, the grains will be under-etched and thus result in age estimates that are too young. If the tracks are over-etched, it will be impossible to count the fission tracks. The etching response of zircons largely depends on the amount of accumulated α-radiation damage, with "older" zircons having medium to low U concentrations needing shorter etch times than "younger" zircons with high U concentrations. Figure 1.10 shows the U concentration and zircon fission-track age relationship of detrital zircons from the European Alps (Bernet et al. 2004a) and it becomes obvious that "old" zircons with high U concentrations tend to be above the countable limit because such grains are commonly metamict and the track densities are too high to distinguish individual tracks, whereas "young" zircons with low U concentrations tend to be under-etched and no tracks are visible (zero-track grains). Although zero-track grains are commonly analyzed in apatite fission-track studies, such grains are not analyzed in zircon fission-track studies because of the complicated etching procedure. Zircon etching requires us to proceed by several etching steps in order to obtain an optimum of well-etched grains, for which the fission tracks are countable. After each etching step, the grain mounts are controlled with an optical microscope for monitoring the advance

of the fission-track etching and eventually it is decided that etching is terminated. All of the etching steps should be protocolled for all samples.

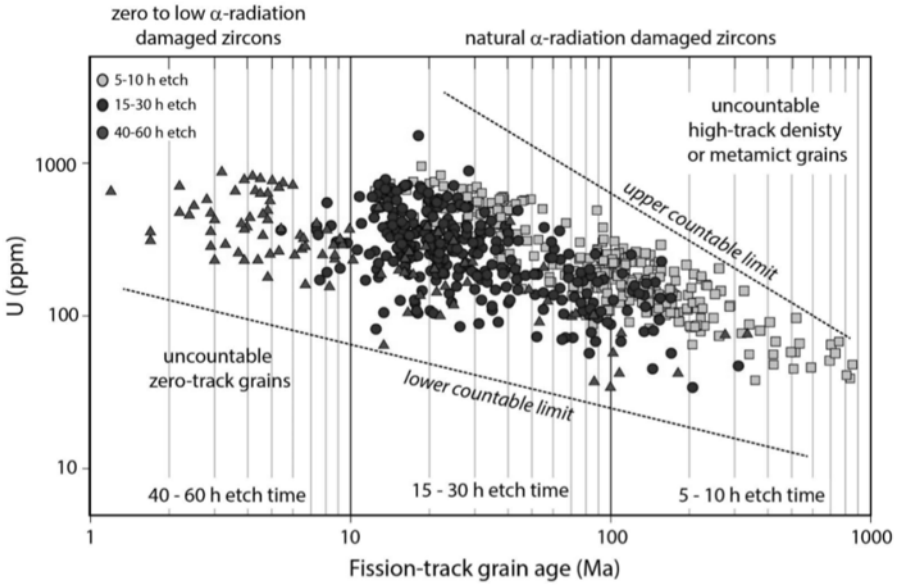

Figure 1.10. *Zircon fission-track age versus U content in relation to etch time (modified from Bernet and Garver (2005)). The upper and lower countable limits delineate the range of apparent cooling ages and U concentrations that can be obtained by fission-track dating. Young low-U and old high-U grains fall outside the detection limits of this method. Over 1000 data points of detrital zircons from New Zealand, European Alps, Apennines, Himalayas and the Mississippi drainage. For a color version of this figure, see www.iste.co.uk/jolivet/fission.zip*

Montario and Garver (2009) extended the countable limit of fission tracks of high track-density grains using a scanning electron microscope technique instead of an optical microscope and counted only etch pits, but this approach was so far not repeated by other labs. Despite these complications, Figure 1.10 shows that for most Cenozoic and Mesozoic orogenic systems or sedimentary basin studies, moderate etch times between 10 and 30 h will be sufficient to reveal countable fission tracks in zircons with apparent cooling ages between 10 and 100 Ma. When dealing with zircons from very rapidly

exhuming areas such as the Himalayan syntaxes, Taiwan, or the Southern Alps of New Zealand, much longer etch times of 40 to > 100 h may be needed to reveal countable fission tracks, as such zircons may have cooling ages of < 5 Ma and have not yet accumulated significant amounts of α-radiation damage.

1.3.2. *External detector method*

Once the fission tracks have been properly etched, the apatites or zircons are in principal ready for fission-track analysis. Not all tracks visible in a grain will be counted but rather a certain count area is defined for which the track density (number of tracks per surface area) is determined (Figure 1.11). In order to calculate an apparent fission-track cooling age, not only the number of tracks or track density is needed, but also the U concentration of the grain over the area where the tracks were counted. Two techniques are nowadays commonly used in fission-track dating for determining the U concentration, the more classical EDM and the still relatively new laser ablation inductively coupled-plasma mass-spectrometry (LA-ICP-MS) approach. The population method, which had been applied by certain laboratories mainly in the 1960s to the 1990s, is nowadays rarely used and not recommended here. Both the EDM and LA-ICP-MS approaches have their own advantages and disadvantages, but one of these techniques needs to be selected in order to determine the U concentration of the analyzed apatites and zircons. The LA-ICP-MS method for fission-track dating is presented in detail in Chapter 3 by Nathan Cogné of this book and will not be explained here. We will only focus on the EDM.

The EDM (Fleischer et al. 1964; Naeser and Dodge 1969) has been widely used by fission-track laboratories around the world as the preferred method over the past 60 years. This method requires an external detector, usually a low-U muscovite sheet, to be attached to the grain mount and the samples are sent together with age standards and dosimeter glasses to a well thermalized research reactor for irradiation with thermal neutrons. The thermal neutron activation causes induced fission of ^{235}U isotopes in the apatite or zircon crystals and creates an image of the crystal in the mica

detector (Figure 1.11). The track density of the induced fission tracks in the mica detector will depend on the U concentration of the crystal and the neutron fluence during irradiation, which in turn will depend on the duration of the irradiation. As zircons have higher U concentrations than apatites, they will be irradiated for a shorter time. Common irradiation durations for zircons are about 1 min and about 11 min for apatites, but this may widely vary between different reactors. Neutron fluence is monitored for each irradiation package with dosimeter glasses of known U concentration (Figure 1.11(A); Table 1.3). Using ^{235}U as a proxy for the ^{238}U concentration works because the isotopic ratio between ^{235}U and ^{238}U is stable in nature at 7.2527×10^{-3} (e.g. Wagner and Van den haute 1992).

Age standards	Age	Mineral
Buluk Member Tuff	16.4 ± 0.2 Ma	Zircon
Fish Canyon Tuff	27.8 ± 0.5 Ma	Apatite, zircon
Durango	31.4 ± 0.5 Ma	Apatite
Mt Dromedary Igneous Complex	98.7 ± 0.6 Ma	Apatite, zircon
Dosimeter glasses	**U (ppm)**	
IRMM540R	15.0 ± 0.9	
IRMM541	49.4 ± 2.7	
CN1	39.8 ± 0.7	
CN2	36.5 ± 1.4	
CN5	12.2 ± 0.6	

Table 1.3. *Commonly used fission-track age standards and dosimeter glasses*

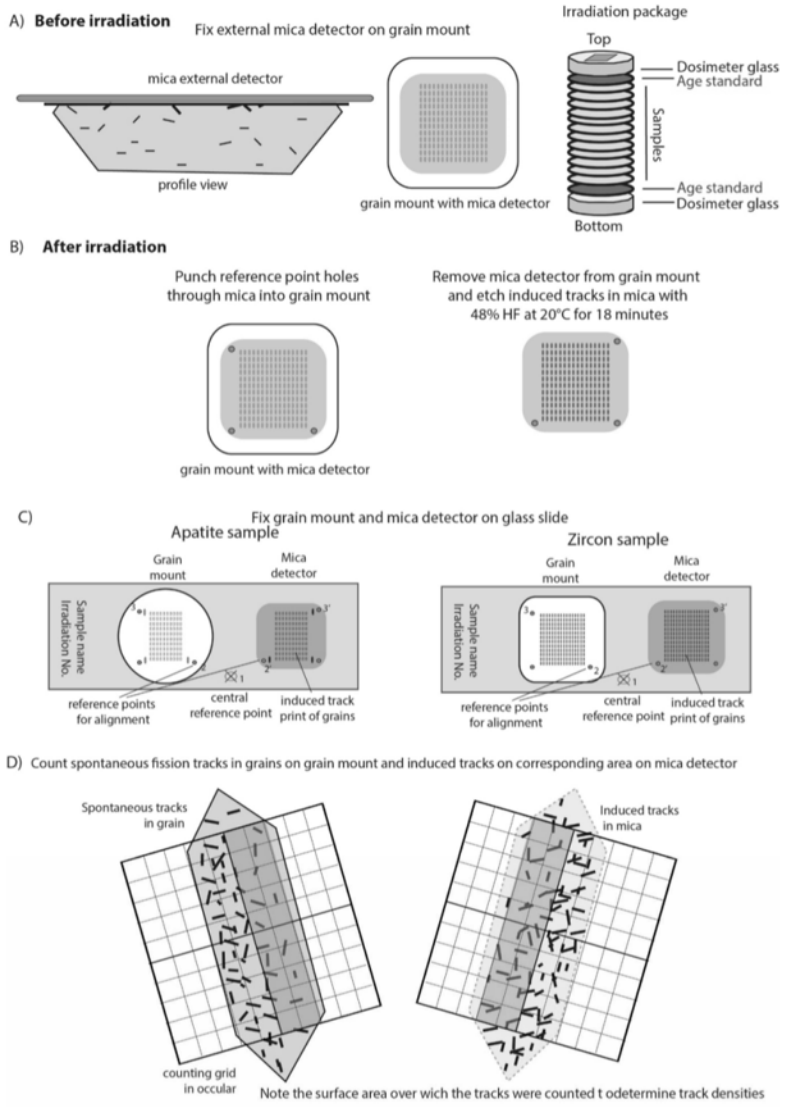

Figure 1.11. *External detector method: (A) mounting of external mica detector on grain mount and organization of samples, age standards and dosimeter glass in irradiation package. (B) Placing of reference points on mica and grain mount, followed by etching of mica detectors to reveal induced tracks. (C) Mounting of grain mount and mica detector on glass slide for analysis with an optical microscope. (D) Counting of spontaneous tracks (Ns) on a selected grain surface and counting of induced tracks (Ni) on the corresponding surface area on the mica detector. For a color version of this figure, see www.iste.co.uk/jolivet/fission.zip*

It is recommended to irradiate age standards (Table 1.3) with each irradiation package in order to determine the zeta calibration factor for each fission-track analysist (see Hurford 1996). After irradiation, the position of the mica detectors on the grain mounts is marked with three reference points to assure proper alignment between the grain mounts and the micas later on during analysis, and the induced fission tracks in the mica detectors are etched at 20°C for 18 min in 48% HF (Figure 1.11(B)). Finally, the grain mounts and mica detectors are fixed on glass slides and are ready for analysis with an optical microscope usually at between 1,000 and 2,000 × magnification (Figure 1.11(C)). The idea is to determine the density of spontaneous fission tracks (ρs) in the grain over a certain surface area and the density of induced tracks (ρi) over the corresponding surface area on the external detector (Figure 1.11(D)). The track counts *Ns* (number of spontaneous tracks in the grain) and *Ni* (induced tracks in the detector) are noted as well as the surface area that was analyzed. The surface area is commonly determined by a 10 × 10 grid of squares of known size in one of the oculars of the microscope, but if counting is done on a computer screen the size of the surface area may be determined with an image processing software.

1.3.3. *Track lengths measurements and track lengths distributions*

As spontaneous fission tracks can form in any direction within the 3D crystal structure, fission tracks may intersect at different angles and the internal surface produced during polishing of the crystals. In order to measure the length of fission tracks, we must find horizontally confined tracks that are in connection with the surface during etching either through other tracks, crystal defects, fractures or cleavage, along which the etchant can enter the crystal and etch the latent horizontal track at depth (Figure 1.12(A)). Horizontally confined tracks are rare, depending on the thermal history and U concentration of the grain. Therefore, many grains need to be checked to obtain if possible up to 100 or more track lengths measurements per sample. Many fission-track laboratories also use a ^{252}Cf irradiation procedure on extra grain mounts in order to add many additional holes to the grains before the etching in order to increase the chance of finding horizontally confined tracks during etching. Of course, such grain mounts cannot be used for age determinations.

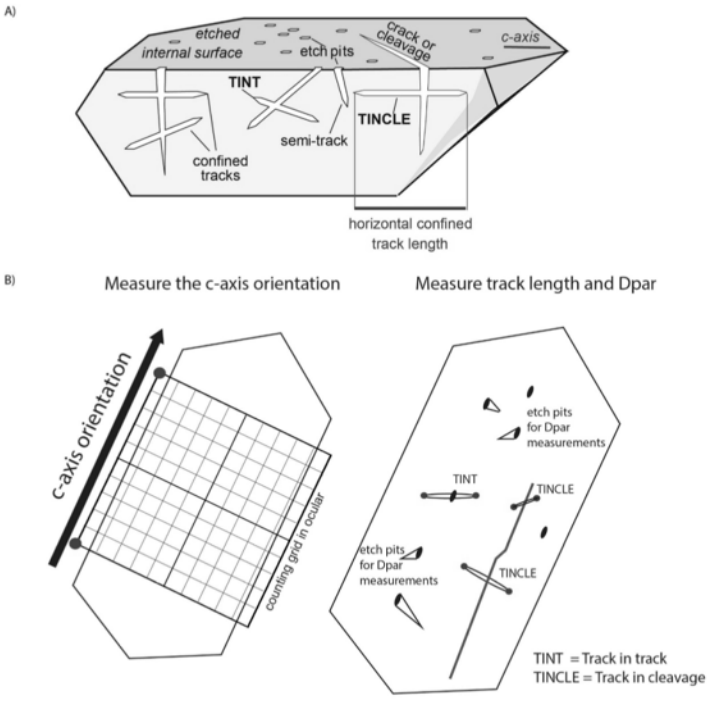

Figure 1.12. *(A) Schematic sketch of polished apatite grain with etch pits, semi-tracks, cleavage, confined tracks. TINT: track in track; and TINCLE: track in cleavage; modified from Hurford (2019). (B) Measurement of c-axis orientation, horizontal confined tracks and Dpar. For a color version of this figure, see www.iste.co.uk/jolivet/fission.zip*

The actual measurement of the length of a horizontally confined fission track in apatite is fairly simple with either the use of a digitizing tablet or through a camera system directly on a computer screen. As the annealing of fission tracks in apatite is anisotropic with respect to track orientation in relation to the crystal c-axis orientation (e.g. Carlson et al. 1999; Donelick et al. 2005), track length measurements in apatite should only be done on crystals mounted parallel to the c-axis. It is necessary to measure not only the track length, but also the angle between the track orientation and the crystal c-axis orientation (Figure 1.12(B)). As the crystal chemistry of apatites also has an influence on track annealing, as mentioned above, it is important to know if we are dealing with fast annealing F-apatites or more slowly annealing Cl-apatites. The chemistry of a crystal can be determined by microprobe analysis, which of course requires additional equipment and

analytical time. Many laboratories today opt for measuring the size of fission-track etch pits oriented parallel to the c-axis, called Dpar, of the same apatite crystal. Dpar is not a direct indicator of the chemical composition of the apatite crystal, but a positive correlation of Dpar size and Cl-content, or a negative correlation of Dpar size and F-content has been observed (Carlson et al. 1999; Donelick et al. 2005). As a general indication, apatites with Dpar values < 1.75 μm tend to be F-rich apatites that anneal more rapidly and at lower temperatures than Cl-rich apatites with Dpar values > 1.75 μm and up to 3 or 4 μm (see a summary on all of this in Donelick et al. 2005). The Dpar values, if possible three to four measurements for every apatite track length measurement, are an independent kinematic parameter that is used together with track lengths measurements and the fission-track grain age data for thermal history modeling (Figure 1.13), using software such as HeFTy (Ketcham 2005), QTQt (Gallagher 2012) or PeCube (Braun 2003; Braun et al. 2012). See Chapter 2 by Kerry Gallagher for more information on modeling.

The initial track length of non-annealed tracks in a Durango apatite, which is one of the most commonly used reference materials in apatite fission-track dating, is on average ~ 16.3 μm. The measurement of track lengths in Durango apatites can therefore be used for calibration purposes, as recommended by Ketcham et al. (2015, 2018). The lengths measurements of non-annealed tracks or tracks that have shortened by ~ 30 or 40% to lengths of 10–9 μm is relatively easy. However, the more the tracks have been affected by annealing and the shorter they are, the more difficult it becomes to recognize horizontally confined tracks and track lengths values below 5 μm are usually not measured. Nonetheless, track lengths measurements are indispensable for thermal history modeling.

Although track length measurements are common practice in apatite fission-track dating, it is rarely done in zircon fission-track dating, because so far, the annealing kinetics of fission tracks in zircon, particularly in relation to the amount of accumulated α-radiation damage, are still poorly understood. Nonetheless, the work by Tagami et al. (1998) and Yamada et al. (1995, 2007) showed that the initial track length of fission tracks in zircon is ~ 11.2 μm and that zircon fission tracks also experience partial annealing over a certain temperature range to full annealing at high temperatures (Figure 1.4). A recent study using track lengths measurements in zircons was presented by Rahn et al. (2019).

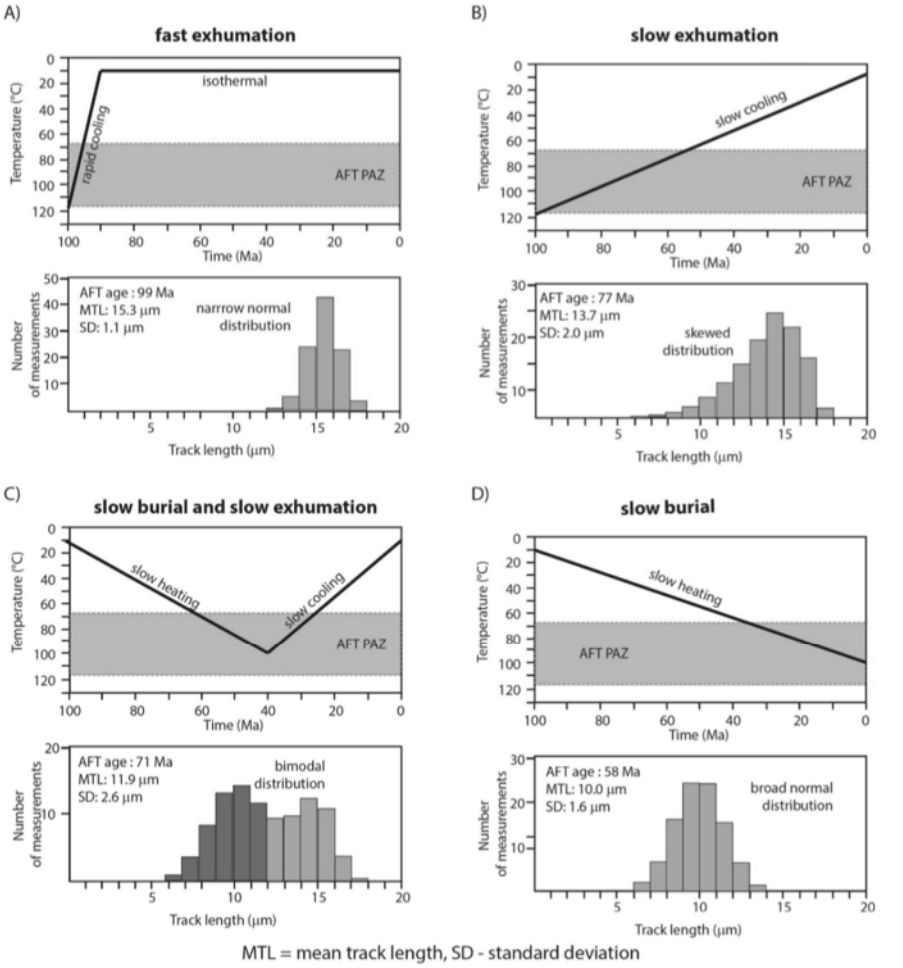

Figure 1.13. *Track lengths distributions and thermal histories (after Gallagher et al. (1998)). For a color version of this figure, see www.iste.co.uk/jolivet/fission.zip*

NOTE ON FIGURE 1.13.– *(A) The simple case of fast exhumation and isothermal conditions at or near the surface since around 90 Ma. The apparent apatite fission-track cooling age could indicate the start of rapid cooling or a tectonic event between 100 and 90 Ma. (B) The case of slow monotonic cooling during slow exhumation. Note that the apparent*

apatite fission-track cooling age does not relate to any rapid cooling or tectonic event. (C) Burial and exhumation controlled thermal history of sediments experiencing burial heating for about 60 Myr followed by 40 Myr of cooling. Burial heating did not exceed the high-temperature limit of the partial annealing zone. Therefore, part of the post-cooling thermal history is preserved in the track lengths data (bimodal distribution). Again, the apparent apatite fission-track cooling age does not relate to any rapid cooling or tectonic event. (D) The case of a borehole sample taken at 3 to 4 km depth, depending on geothermal gradient. Strong shortening of tracks. The apparent fission-track cooling age is strongly affected partial annealing and has no geological meaning.

1.4. Statistics of fission-track dating

1.4.1. *Age equation, pooled age, central age, χ2-test and age dispersion*

The underlying statistics for the EDM have been carefully developed since the 1960s and were summarized by Wagner and Van den haute (1992), Galbraith (2005), Hurford (2019) and Vermeesch (2019). Here, we will touch only on some of the most important aspects. For more detail, an interested reader should consult Galbraith (2005).

The formation of spontaneous fission tracks in U-bearing minerals follows a Poisson distribution, which means that one spontaneous fission event is independent of another spontaneous fission event. The same is the case for the formation of the induced tracks during irradiation. Furthermore, the frequency of the occurrence of spontaneous fission events of ^{238}U in a crystal depends on the spontaneous fission-decay constant $\lambda_f \sim 7.5 \times 10^{-17}$ a^{-1} and the U concentration of the crystal (Wagner and Van den haute 1992; Donelick et al. 2005).

For the EDM, a fission-tack age will be calculated from the ρs/ρi track density ratios using equation [1.4]:

$$t = \frac{1}{\lambda} \ln\left[1 + \frac{\lambda \zeta \rho_s c \rho_d}{\rho_i}\right] \qquad [1.4]$$

where λ is the total decay constant of ^{238}U decay by α-decay ($\lambda\alpha$) and spontaneous fission decay (λf). The decay constant can be related to the half-life ($T_{1/2}$) shown in Table 1.1, by equation [1.5]:

$$T_{1/2} = 0.693/\lambda \quad [1.5]$$

The zeta calibration factor (ζ) is calculated using equation [1.6], ρd is determined from track counts of the dosimeter glasses external detectors, and c is a geometry factor of 0.5, given that half of the crystal was removed by polishing.

The zeta calibration factor is determined from analysis of age standards of known age. Commonly used standards in fission-track dating are the Durango Tuff and Fish Canyon Tuff for apatites, and the Fish Canyon Tuff and Buluk Tuff for zircons (Table 1.3).

$$\zeta = \frac{e^{\lambda_D t_{std}} - 1}{\lambda_D \left(\rho_s/\rho_i\right)_{std} c \rho_d} \quad [1.6]$$

In equation [1.6], t_{std} is the age of the standard and $(\rho s/\rho i)_{std}$ are the track densities of the grains and micas of the standards.

A simple symmetrical error for the fission-track age can be calculated using equation [1.7]:

$$\sigma_i = \left[\frac{1}{N_{s,i}} + \frac{1}{N_{i,i}} + \frac{1}{N_d} + \left(\frac{\sigma_\zeta}{\zeta} \right)^2 \right]^{\frac{1}{2}} \quad [1.7]$$

where Ns is the number of the spontaneous fission-track counts, Ni is the number of the induced fission-track counts, Nd is the number of the fission-track counts of the fluence monitor, ζ is the zeta value and σ_ζ is the error of the zeta value. This equation shows that the higher the number of track counts, the smaller the error of the age estimate becomes statistically. Fission-track ages based on low track counts tend have a larger uncertainty than the same fission-track age based on high track counts (Figure 1.14). This is why it is important to count fission tracks over large areas, if possible, to increase the number of tracks counted.

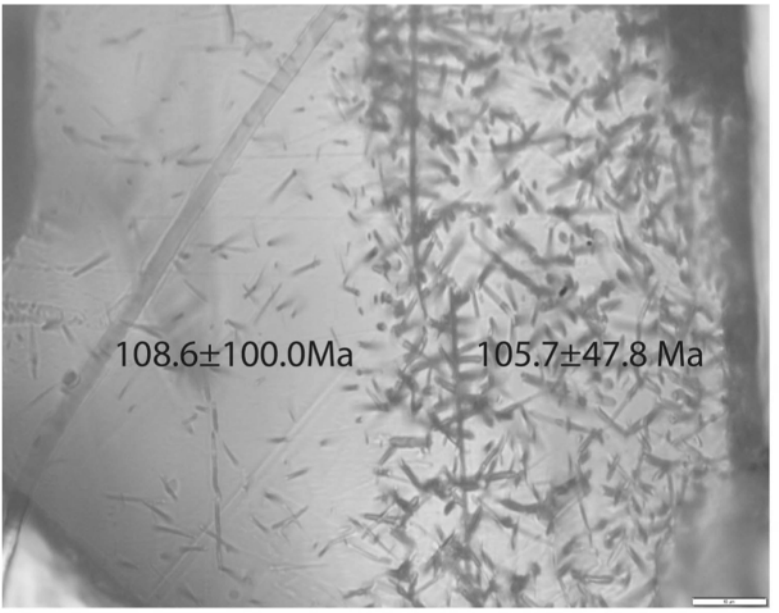

April 10 2019 15:28 *BinomFit for Windows ver.1.2* *Page 1*
Datafile: C:\Fission-track Lab\irradiations\2018\9-2018_zircon\San Lucas\16SLAZ01B_9-2018-14_two_grains.ftz
Title: 16SLAZ01B_9-2018-14 two grains

NEW PARAMETERS - ZETA METHOD

EFFECTIVE TRACK DENSITY FOR FLUENCE MONITOR (tracks/cm^2): 3.71E+05
RELATIVE ERROR (%): 1.25
EFFECTIVE URANIUM CONTENT OF MONITOR (ppm): 50.00
ZETA FACTOR AND STANDARD ERROR (yr cm^2): 131.49 5.30
SIZE OF COUNTER SQUARE (cm^2): 6.39E-07

GRAIN AGES IN ORIGINAL ORDER

Grain no.	RhoS (cm^-2)	(Ns)	RhoI (cm^-2)	(Ni)	Squares	U+/-2s	Grain Age (Ma) Age	--95% CI--	
1	3.21E+06	(41)	7.04E+05	(9)	20	95 62	108.6	52.9	254.8
2	9.62E+06	(123)	2.19E+06	(28)	20	296 111	105.7	70.1	165.7
POOLED	6.42E+06	(164)	1.45E+06	(37)	40	195 64	106.8	74.7	157.0

CHI^2 PROBABILITY (%): 93.2

POOLED AGE W/ 68% CONF. INTERVAL(Ma): 106.8, 88.1 -- 130.4 (-18.6 +23.7)
95% CONF. INTERVAL(Ma): 74.7 -- 157.0 (-32.0 +50.3)

CENTRAL AGE W/ 68% CONF. INTERVAL(Ma): 107.1, 89.0 -- 128.9 (-18.1 +21.8)
95% CONF. INTERVAL(Ma): 74.5 -- 153.9 (-32.7 +46.8)
AGE DISPERSION (%): 0.0

Figure 1.14. *Example of high and low track count areas within one zircon grain with strong U zonation. In both, the low-track density and the high-track density part of the grain the apparent zircon fission-track cooling age is the same at about 107 Ma, but the more tracks can be counted statistically the error is smaller. The table below the image shows the track counts, single ages, pooled age, central age, χ^2 probability and age dispersion, all calculated with the Binomfit program of Brandon (see Ehlers et al. (2005))*

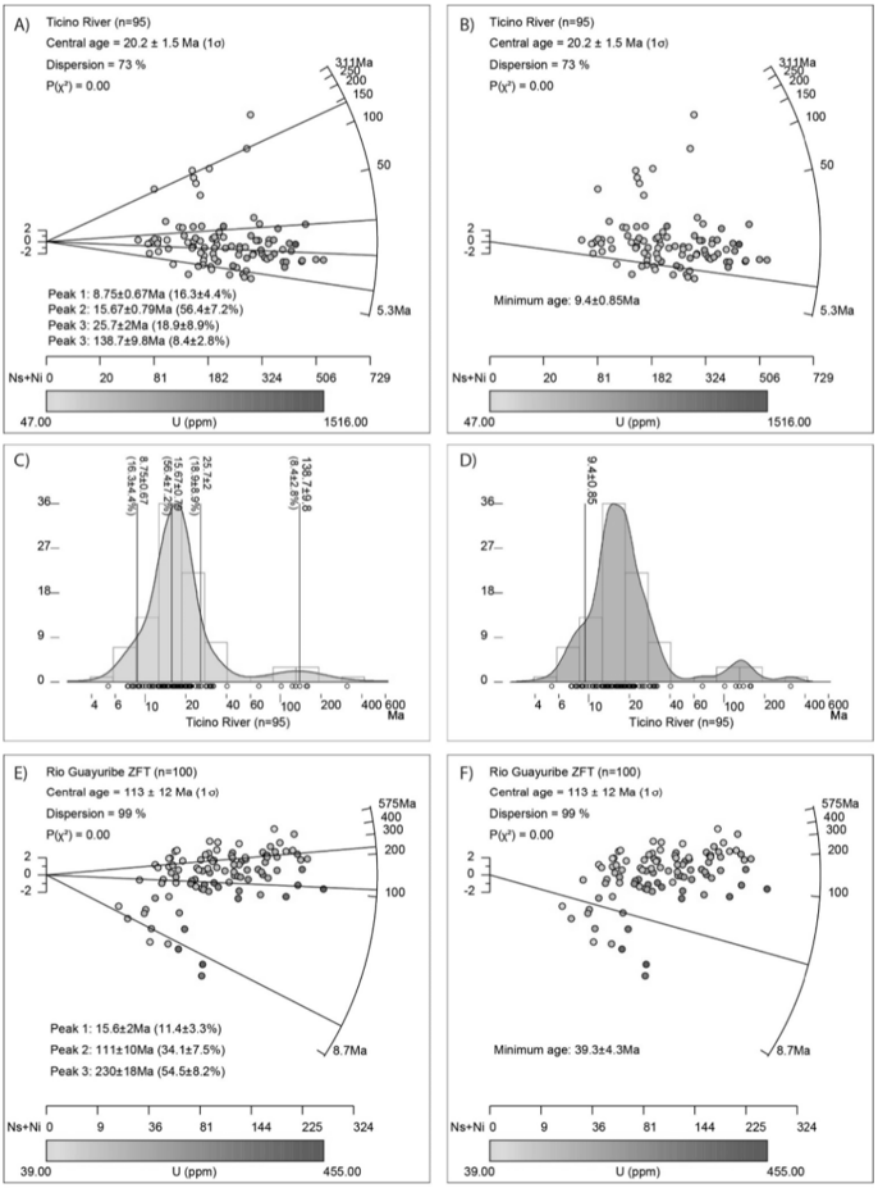

Figure 1.15. *Example for data presentation of detrital fission-track data, here with the Ticino River detrital zircon fission-track data from Bernet et al. (2001). For a color version of this figure, see www.iste.co.uk/jolivet/fission.zip*

NOTE ON FIGURE 1.15.– *(A) radial plot with four age peaks. (B) Radial plot with minimum age. (C) Kernel density estimate plot with four age peaks. (D) Probability density plot with minimum age estimate. (E) Radial plot with peak ages of the Rio Guayuribe sample (data from Urueña et al. 2019). (F) Radial plot with minimum age estimate of the Rio Guayuribe sample. All plots were made with the RadialPlotter program of Vermeesch (2009).*

The data analysis steps recommended by Galbraith (2005) for fission-track data are to check the single grain age data and plot them in a radial plot to visualize the spread of the age distribution (Figures 1.15(A) and (B)). Less commonly used plots for presenting detrital fission-track data are kernel density estimate plot or probability density plots (Figures 1.15(C) and (D)). Based on the *Ns* and *Ni* counts of each grain in a sample, the χ^2 homogeneity test of equation [1.8] should be applied to see if the observed grain age distribution is consistent with one common true age, or if a possible continuous or discrete mixture of ages exists.

$$x^2_{stat} = \frac{1}{N_s N_i} \sum_{j=1}^{n} \frac{(N_{sj} N_i - N_{ij} N_s)^2}{N_{sj} + N_{ij}} \qquad [1.8]$$

The general rule is, if the $P(\chi^2)$ is >> 0.05, it is relatively certain that only one common true age is represented by the grain age distribution. If the $P(\chi^2)$ is < 0.05, then it is possible that more than one age population constitutes the grain age distribution of the sample. If the P (χ^2) is < 0.01, it is very likely that more than one age population is present. In addition, we need to calculate the age dispersion. If the age dispersion has values of 20% or less, then it is very likely that only one common true age is present, but if the age dispersion shows values >> 20% it is almost certain that more than one age population is present (Figure 1.15).

Finally, an estimate of the average fission-track age of the sample is calculated, which is either presented as the pooled age or the central age and their precisions. The pooled age is calculated like a single grain age, but it simply pools all of the *Ns* and *Ni* counts and treats the sample basically as one large grain. If the single grain age distribution fails the χ^2 test and the age dispersion is > ~ 20%, it is recommended to use the central age instead of the pooled age as an estimate of the sample average age. The central age calculation was developed by Galbraith and Laslett (1993) and requires an iterative solution. Software packages such as Binomfit of Brandon (see Ehlers et al. 2005) or RadialPlotter of Vermeesch (2009) will do these calculations conveniently. For over-dispersed grain-age distributions, the central age is

regarded as a statistically more sound average age estimate than the pooled age (Vermeesch 2019). Because the central age is exactly the same as the pooled age if the age dispersion is low, many labs now only use the central age. In detrital thermochronology studies, the objective is to date about 100 grains per sample, and it is common to have samples with grain age distributions that fail the χ^2 and have large ($> \sim 20\%$) age dispersion values. The question is what causes age dispersion in detrital samples? This question will be addressed in the following sections.

1.5. Detrital thermochronology

1.5.1. *Continuous and discrete mixtures of detrital cooling ages*

As mentioned above, detrital thermochronology refers to the thermochronological analysis of detrital grains collected either from modern river and beach sediments or from ancient sandstone. In the case of a modern river or beach sediment, over-dispersion of grain ages may reflect the continuous or discrete mixture of a large range of grain ages derived from different bedrock source areas with individual cooling histories (Figures 1.15 and 1.16). This is common for samples collected in distal locations, having large regional drainage areas, as shown in the Rhone delta zircon fission-track data (Figure 1.16) (Bernet et al. 2004b).

The Rhone delta zircon fission-track data reflect orogenic exhumation of the Western and Centrals Alps with Alpine cooling ages < 35 Ma (timing of collision and major regional metamorphism, peaks 1–3), and recycling of partially (peak 4) and non-reset (peak 5) cover units and a ~ 20% sediment contribution from the Massif Centrale (peak 3 and 5) (see van Andel (1955); Bernet et al. (2004b)). At least for modern sediment samples, we do not have to worry about partial annealing during burial-heating. If partial annealing is detected, for example through track length measurements, then it is inherited from the thermal history of the sediment source area. Slow cooling of the source rock through the fission-track PAZ or reheating to partial annealing temperatures and subsequent renewed cooling during erosional exhumation of the source rock may cause that partially annealed grains are already derived from the source rock and may result in an over-dispersed continuous mixture of grain ages in the modern sediment sample. In contrast, detrital apatites and zircons from ancient sandstone collected from either drill cores or from outcrops of inverted basins may have been subjected to partial annealing during burial, which may also contribute to over-dispersion of the observed grain age distribution (see below).

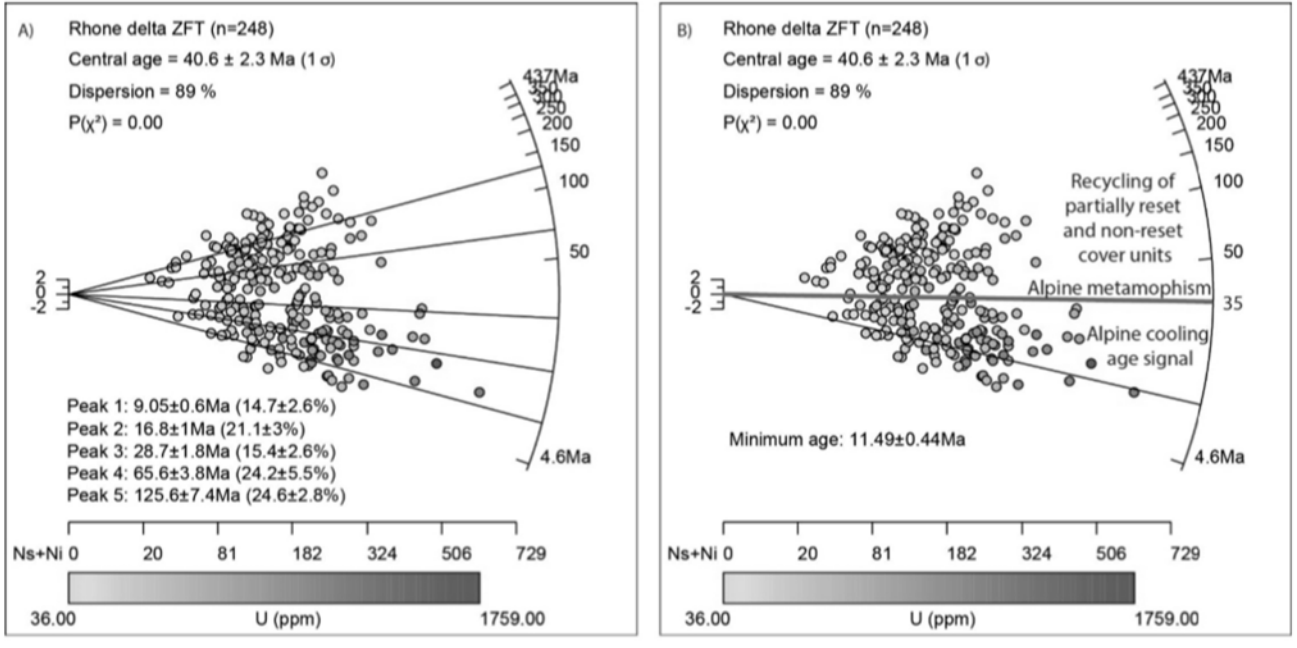

Figure 1.16. *Radial plot of the Rhone delta zircon fission-track data with (A) age peaks and (B) minimum age (data from Bernet et al. (2004b)). All plots were made with the RadialPlotter program of Vermeesch (2009). For a color version of this figure, see www.iste.co.uk/jolivet/fission.zip*

1.5.2. *Peak fitting and minimum age model*

Depending on the objective of the study (e.g. provenance analysis, exhumation rate determination, basin thermal history analysis as discussed below), it is possible to test statistically if different discrete grain ages populations are present in a detrital sample by using the peak fitting routines, available in the Binomfit program of Brandon (see Ehlers et al. (2005)) or the RadialPlotter program of Vermeesch (2009), in order to separate different populations or peaks. The challenge is to know how many peaks should be fitted to the observed grain age distribution. As for any numeric modeling in the geosciences, geological constraints should have the highest priority for constraining the models and the interpretation. For peak-fitting, it is recommended to inspect the results to see if they are geologically meaningful and by how much individual peaks overlap or if they are well separated (Figures 1.15(A) and (E) and 1.16(A)). Furthermore, we have to keep in mind that the number of dated grains will have an important influence on how many peaks can be fitted, as it is easier to fit more peaks when more grains were analyzed, even if these peak ages may not have any geological meaning (Vermeesch 2019). The Binomfit program uses an F-test between different solutions to obtain the best-fit solution of peaks (Ehlers et al. 2005). With the RadialPlotter program of Vermeesch (2009), it is not quite clear how the automatic peak-fit function determines how many peaks should be fitted. At any rate, peak-fitting should only be done if necessary (e.g. for provenance studies for comparison to bedrock data sets of the source area), and the interpretation should always be cautious, as particularly older age peaks may not reflect any specific tectonic or exhumation events or episodes of rapid cooling. The safest bet is to focus on the youngest or two youngest age peaks in detrital samples, if they do not significantly overlap, and if the purpose is to determine the most rapid exhumation rates in the sediment source area. But again, sample size may bias the results, and larger data sets tend to have younger first and second age peaks (Naylor et al. 2015; Vermeesch 2019). A suitable alternative may be to focus on the central age for obtaining a sample average exhumation rate estimate, and on the minimum age for determining maximum exhumation rates in the drainage area.

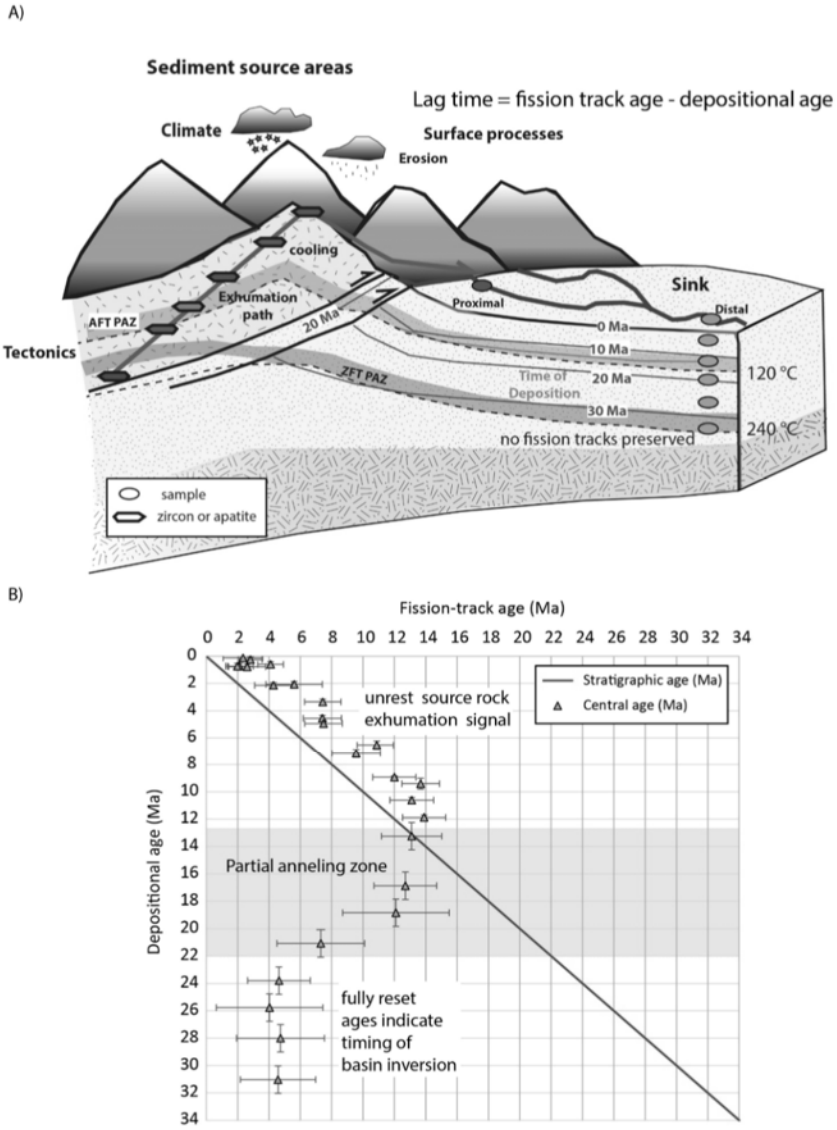

Figure 1.17. *(A) Lag-time concept (modified from Bernet (2019)). (B) Potential trend of no annealing, partial annealing or full annealing of fission tracks and associated reset apparent cooling ages with increasing heating during burial within a sedimentary basin. For a color version of this figure, see www.iste.co.uk/jolivet/fission.zip*

The minimum age was also introduced by Galbraith and Laslett (1993), and it presents an estimate of the first coherent age component in an observed grain age distribution, while avoiding the sample size bias to younger ages by peak-fitting (Figures 1.18(C) and (D)) (Vermeesch 2019). Comparing the minimum age estimate presented here for the Ticino River, Rio Guayuribe and the Rhone delta (Figures 1.15(B) and (F) and 1.16(B)) in comparison to the youngest peak age (peak 1) of the same data sets shown in Figures 1.15(A) and (E) and 1.16(A), we can see that the minimum age estimate may be significantly older than peak 1, if the overall grain-age distribution is dominated by older grains.

1.5.3. *Recognizing partial and full annealing in detrital fission-track data sets*

As long as detrital apatites and zircons have not been affected by partial annealing because of burial heating in sedimentary basins, their grain age distributions reflect the source area exhumation history and they can be used as sediment provenance indicators (e.g. Hurford et al. 1984; Cerveny et al. 1988; Carter 1999; Spiegel et al. 2000; Bernet et al. 2004a, 2004b; Bermúdez et al. 2013, 2017; Malusà and Fitzgerald 2020). By collecting samples from basin sedimentary rocks at different stratigraphic levels, the long-term exhumation history of a mountain belt can be reconstructed (Garver and Brandon 1994a, 1994b; Bernet et al. 2001, 2009). For this, the stratigraphic age has to be known from independent magneto- and biostratigraphic constraints or absolute dating of volcanic ash layers. In the simplest case, and the absence of post-depositional partial annealing, all of the single grain age, minimum ages, peak ages or central ages determined for the detrital sample are older than the depositional age. Interpretation of the data is straight forward, and the difference between the minimum age or the central age and the depositional age can be used to calculate the lag time (fission-track age minus the depositional age). The lag-time concept is shown in Figure 1.17(A). During exhumation through the upper crust because of erosion at the surface or because of normal faulting, apatite and zircon crystals will cool below the *Tc* and through the PAZ of each of the two dating techniques. The lag time of the minimum age of a detrital sample can be transferred into an estimate of the fastest exhumation rates in the drainage area (see below), whereas the central age lag time may provide an estimate on drainage basin average exhumation rates (Garver et al. 1999; Bernet and Garver 2005; Bernet 2019).

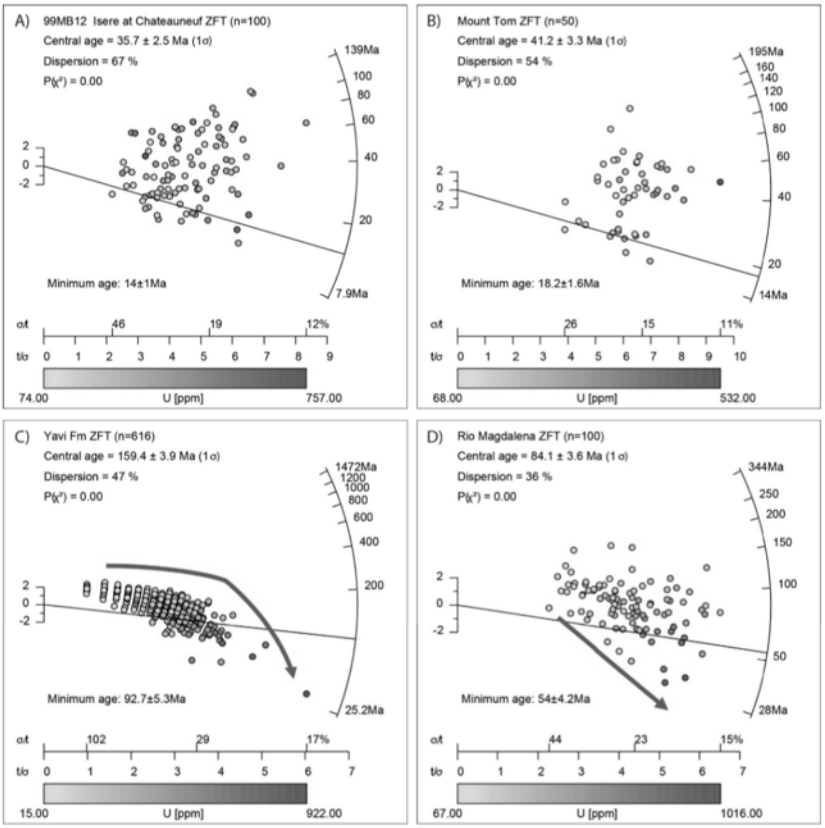

Figure 1.18. *(A) Radial plot with minimum age of the Isère River, France (Bernet et al. 2004b). The grain age distribution does not show signs of a partially annealed zircon fission-track ages, as no clear fission-track age–U-content trend emerges. (B) Radial plot of detrital zircon fission-track data of late Miocene French foreland basin deposits (sample 99MB13 from Bernet et al. (2009)). The peak ages and the central ages are much older than the age of deposition and the distribution of grain ages shows no signs of partial annealing. The minimum age of this sample is 17.43 ± 0.9 Ma. (C) The combined dataset of the Early Cretaceous Yavi Formation in the Upper Magdalena River Valley basin, Colombia (Roncancio 2014), shows a clear partial annealing trend with high-U grains giving the youngest cooling ages (red arrow). (D) The age distribution in the modern Magdalena River sediments (Urueña et al. 2019) shows that the inherited partial annealing signal of the Yavi Formation is recycled into the modern river sediments of the Magdalena River drainage basin. All plots were made with the RadialPlotter program of Vermeesch (2009). For a color version of this figure, see www.iste.co.uk/jolivet/fission.zip*

Just because a few single grain ages within their two-sigma uncertainties are younger than the depositional age, this is not an indication for partial annealing during burial. If however the minimum age or first peak age are younger than the depositional age, then the apatites or zircons were somewhat affected by partial annealing during burial (Figure 1.17(B)). If the central age is also younger than the depositional age, then partial annealing was relatively strong. In such cases, the fission-track ages themselves do not reflect source area information anymore, even if it may still be possible to fit peaks to such data sets, but these peak ages are most likely meaningless. Samples strongly affected by partial annealing tend to show decreasing age dispersion with a central age significantly younger than the depositional. In this respect, it is of interest to see how the minimum ages of samples from different stratigraphic levels may change or not with increasing (paleo-) depth (Figure 1.17(B)). For samples collected from an inverted basin, it is possible that the observed minimum ages, or first peak ages, or even central ages, line-up around a common age with increasing paleo-depth, indicating the timing of rapid basin inversion (Figure 1.17(B)) (van der Beek 2006). If burial heating was high enough to cause full annealing, the apatites and/or zircons should have zero ages in the case of an active basin with samples collected from a drill hole, or the central or minimum ages should indicate the timing of basin inversion for samples collected from outcrops, if the inversion was rapid.

As mentioned above, zircons that have accumulated considerable amounts of α-radiation damage are more susceptible to partial annealing that grains with the same thermal history but less α-radiation damage. More annealing will result in younger apparent cooling ages. We can check if a specific U-content–fission-track age relationship exists by plotting the single grain age data together with an indication of U-content on a radial plot (Figure 1.18). A non-reset zircon fission-track grain age distribution, such as of the Isère River in France near Chateauneuf-sur-Isère (data from Bernet et al. (2004b)), shows no obvious relationship between zircon fission-track cooling age and U content (Figure 1.19(A)). The same goes for the Miocene foreland basin deposits with a stratigraphic age of 8 Ma, also collected near Chateauneuf-sur-Isère (sample 99MB13 from Bernet et al. (2009)) (Figure 1.19(B)). The peak, central and the minimum age of 17.43 ± 0.9 Ma are all much older than the age of deposition. In contrast, the combined dataset of four samples

from the Early Cretaceous Yavi Formation in the Upper Magdalena River Valley basin between the Central and Eastern Cordillera in Colombia (data from Roncancio (2014)) shows a considerable degree of partial annealing (Figure 1.19(C)). The first two peaks are younger than the depositional age range and the central age is equivalent to the stratigraphic age. The minimum age of 91.3 ± 6.5 Ma is also much younger than the depositional age of about 140–130 Ma and a clear trend of younger grains having higher U concentrations of the grains with younger apparent cooling ages is visible. The Yavi Formation sedimentary rocks are currently being exposed to erosion and the zircons are recycled in the Magdalena River drainage today, as it can be seen in the modern river sediments of the Magdalena River collected near Giradot (Figure 1.19(D), with data from Urueña et al. (2019)).

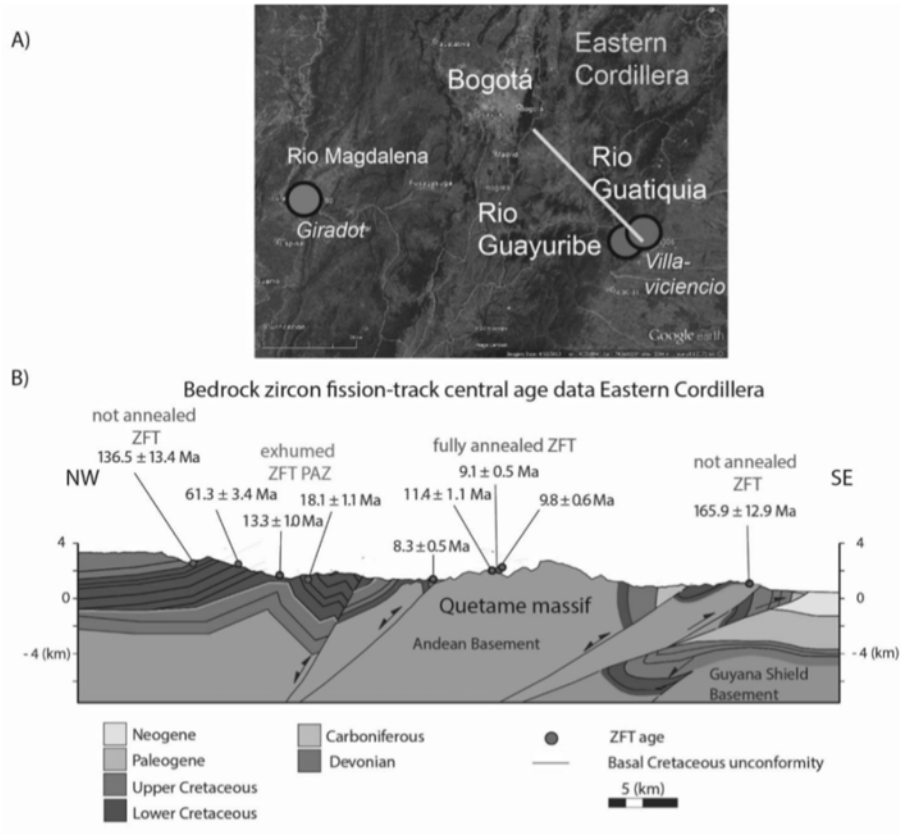

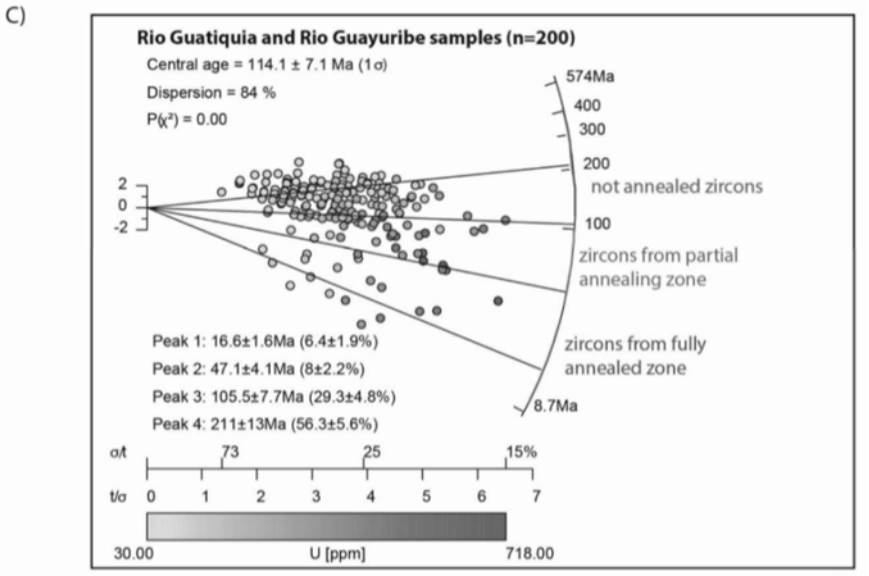

Figure 1.19. *(A) Map of the Eastern Cordillera in Colombia between Bogotá and Villaviciencio shows the location of the profile and the River sample locations (map from Google Earth). (B) Simplified geological profile through the Eastern Cordillera, showing bedrock zircon fission-track ages (modified from Parra et al. (2009)). (C) Combined detrital zircon fission-track data set of the Rio Guayuribe and the Rio Guatiquia on the eastern flank of the Eastern Cordillera (Urueña et al. 2019). For a color version of this figure, see www.iste.co.uk/jolivet/fission.zip*

1.6. Applications of detrital thermochronology

1.6.1. *Studying source-to-sink relationships*

Many studies over the past decades were dedicated to understanding the interactions between tectonics, climate and surface processes during the evolution of mountain belts, the transfer of sediment to sedimentary basins, and the tectonic, stratigraphic and thermal evolution of sedimentary basins. Sediment provenance analysis plays an important role in such studies, as they allow to determine from where sediments were derived. Fission-track dating of detrital apatite and zircon can help to narrow down source areas (Hurford and Carter 1991; Brandon and Vance 1992; Garver and Brandon 1994a, 1994b; Carter 1999, 2007, 2019; Malusà and Fitzgerald 2020). This

works well in areas such as the European Alps, where a dense data set of bedrock fission-track ages has been published over the years and the detrital grain age distributions or peak ages from modern sediments and ancient sandstones can be compared to the existing bedrock data set (e.g. Spiegel et al. 2000; Bernet et al. 2001, 2004a, 2004b, 2009; Trautwein et al. 2002; Glotzbach et al. 2011). As an example, Figure 2.19 shows a profile of zircon fission-track central ages from mainly Cretaceous sedimentary cover and Andean crystalline basement rocks through the Eastern Cordillera of the Northern Andes in Colombia (Parra et al. 2009). The data trend shows an exhumed zircon fission-track PAZ. The combined modern river zircon fission-track data of the Rio Guayuribe and Rio Guatiquia (Urueña et al. 2019), which drain the same area as shown in the profile, display a faithful image of the drainage basin bedrock cooling age distribution.

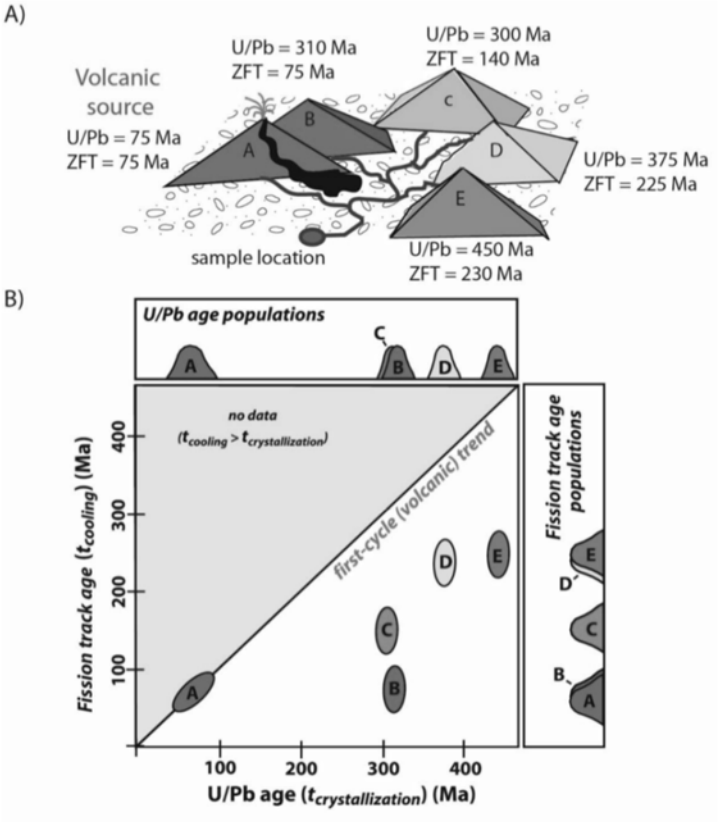

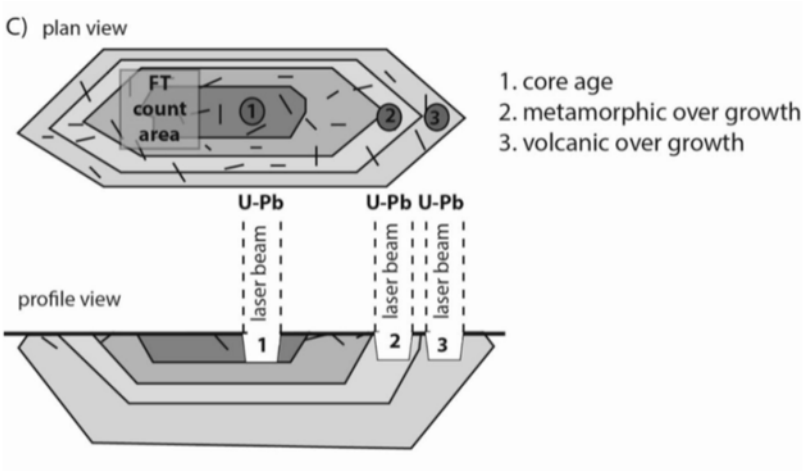

Figure 1.20. *(A and B) Double-dating concept for provenance analysis for discriminating different source areas with either overlapping crystallization ages or overlapping cooling ages (modified from Reiners et al. (2005)). (C) Suggested core-to-rim LA-ICP-MS U-Pb age profile for identifying volcanic zircons, as zircon crystals may even be recycled through magma chambers (e.g. Bernet et al. 2016). For a color version of this figure, see www.iste.co.uk/jolivet/fission.zip*

A major advance in provenance analysis using low-temperature thermochronology was the development of single grain double dating methods. Carter and Moss (1999) and Carter and Bristow (2000, 2003) published the first studies with combined fission-track and U-Pb dating on the same grains. Similarly, double-dating on zircon was done with (U-Th)/He and U-Pb dating (Rahl et al. 2003; Reiners et al. 2005). The advantage of double-dating is to combine crystallization ages (U-Pb) with cooling ages (FT), which can help us to narrow down source areas (Figure 1.20). This has been done for example on foreland basin sediments of the Himalaya (Bernet et al. 2006), or to trace provenance and exhumation of glaciated areas in the St. Elias Mountains of Alaska (Enkelmann et al. 2009a, 2009b). It can also be applied to identifying the contribution of zircon derived from volcanic activity (Jourdan et al. 2013). However, we need to be careful with where to place the ablation spot on volcanically derived zircons, as the volcanic U-Pb age signal may only be detectable in the rim, with many zircons may having older inherited cores (e.g. Bernet et al. 2016).

With advances in LA-ICP-MS analyses, the same fission-track and U-Pb double dating technique has also been applied to detrital apatite studies

(Mark et al. 2016). Furthermore, double-dating, or even U-Pb, fission-track and (U-Th)/He triple dating (Carrapa et al. 2009), can be combined with geochemical analyses of the same single grains. For example, Sm and Nd isotopic analyses of apatite (Foster and Carter 2007; Carter and Foster 2009) or Lu and Hf isotopic analyses of zircons can improve the provenance interpretation (Carter 2019).

1.6.2. *Exhumation studies*

Fission-track cooling ages of zircon or apatite can be translated into first-order estimates of long-term exhumation rates, using the lag-time concept shown in Figure 1.18. The fission-track age, be it a single grain age, the minimum age, central age or a peak age and its difference to the time of deposition, provides the time elapsed (lag time) between cooling below the *Tc*, exhumation to the surface, erosion, transport and deposition. In active tectonic settings such as in the Alps, the Himalaya or the Andes the time for sediment transport in the drainage system is negligible with respect to the uncertainty of the fission-track age, and therefore regarded as instantaneous on geological time scales. Given the fact that the minimum, central and peak ages group the cooling age information of many different single grain ages, the exhumation or erosion rates determined from such data indicate the order of magnitude. This will also depend on which numerical techniques are used to convert cooling ages into exhumation rates (e.g. Willett and Brandon 2013). One of the simplest approaches is to use a 1D thermal advection model to get an exhumation rate estimate (Figure 1.21(A)). Nonetheless, such a simple approach is based on some simplifying assumptions, which in many cases are not met or at least not known (e.g. steady-state exhumation, constant geothermal gradient, surface temperature at the start of exhumation, etc.). More sophisticated modeling of exhumation rates or exhumation scenarios (e.g. PeCube; Braun 2003) will consider the 3D geometry of the exhumation path and transient thermal conditions in the upper crust during changes of exhumation rates. Furthermore, the interpretation of detrital fission-track data in terms of exhumation rates becomes particularly challenging when approaching very rapid exhumation rates of > 2–3 km/Myr or more, or very slow exhumation rates of < 0.1 km/Myr (Figure 1.21(A)). For such cases, fission-track dating does not have sufficient precision and other dating techniques are needed to complement the fission-track data. Higher temperature thermochronometers, such as ^{40}Ar-^{39}Ar dating of detrital white mica, may provide additional constraints for very rapid exhumation, whereas (U-Th)/He dating of detrital apatite or ^{10}Be terrestrial cosmogenic

nuclide dating of detrital quartz may help us to constrain very slow erosion rates, or determine erosion rates over shorter timescales (tens to hundreds of thousands of years instead of millions of years). For more information on (U-Th)/He dating, see Chapter 4 by Gautheron et al. Switching from slow (e.g. < 0.1 km/Myr) to rapid (> 1 km/Myr) exhumation will cause advection of heat depending on initially low thermal gradients (e.g. 20°C/km) or high (e.g. 50°C/km) thermal gradients (Figure 2.21(B)), which in turn has also an effect on the *Tc* as the cooling rate will change (Figure 1.21(C)), until the system adjusts to new steady-state thermal conditions, if the more rapid exhumation rate is maintained. Similarly, switching from rapid to slow exhumation will cause a relaxation of isotherms, possibly resulting in a rapid cooling signal, even if the system is in fact decelerating (Braun 2016).

One of the first detrital zircon fission-track studies addressing the exhumation of the Western Himalaya was work done by Cerveny et al. (1988) on the modern Indus River and Siwaliks foreland basin sediments in Pakistan. Following the same approach, this work was extended to the Western Himalaya (Chirouze et al. 2015), the central Himalaya in Nepal (Bernet et al. 2006; Chirouze et al. 2012) and the Eastern Himalaya (Stewart et al. 2008; Chirouze et al. 2013; Gemignani et al. 2018). As shown in Figure 1.22, the detrital zircon fission-track exhumation signal along the Himalayan front is fairly constant from the Mid-Miocene to the present, with the highest rates of exhumation observed in the western and eastern syntaxes. A recent study on the exhumation of the Himalaya using detrital apatite fission-track data obtained from Bengal fan drill cores and rivers sediments was published by Huyghe et al. (2020).

In the literature, many other examples exist where detrital apatite or zircon fission-track analysis were used to study the exhumation history of orogenic systems, such as the European Alps (e.g. Spiegel et al. 2000; Bernet et al. 2001, 2009; Glotzbach et al. 2011), the southern Alps of New Zealand (e.g. Garver and Kamp 2002), or the Andes (e.g. Ruiz et al. 2004; Carrapa et al. 2009; Parra et al. 2012; Bermúdez et al. 2013, 2017; Caballero et al. 2013). Most of these studies follow a similar approach, combining provenance information and exhumation rate estimates derived from fission track and additional information. Malusà (2019) and Malusà and Fitzgerald (2020) presented a guide to interpreting complex detrital fission-track datasets, and Fitzgerald et al. (2019) summarized how thermochronological analysis can be applied to pebbles collected from conglomerates.

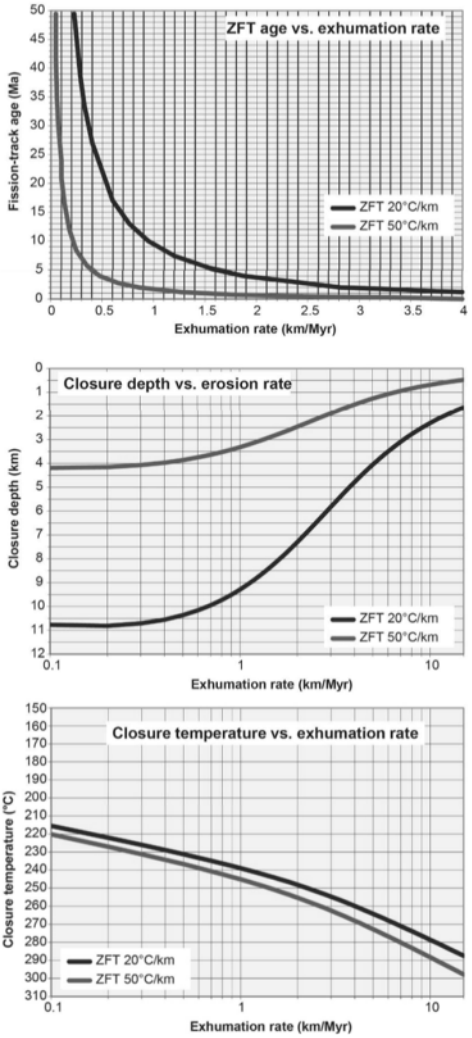

Figure 1.21. *(A) Zircon fission-track age or lag-time versus exhumation rate of natural α-radiation damaged zircons for initial thermal gradients of 20°C/km and 50°C/km. (B) Depth of the closure isotherm (closure depth) versus exhumation rate for initial thermal gradients of 20 and 50°C/km. (C) Zircon fission-track closure temperature versus exhumation rate for initial thermal gradients of 20 and 50°C/km. Data for all plots were calculated with the 1D thermal advection model Age2edot of Brandon (see Ehlers et al. 2005) using a 30 km layer depth to constant temperature as the lower model boundary, a 10°C surface temperature as the upper model boundary, thermal diffusivity of 30 km^2/Myr and an internal heat production of 8°C/Myr. For a color version of this figure, see www.iste.co.uk/jolivet/fission.zip*

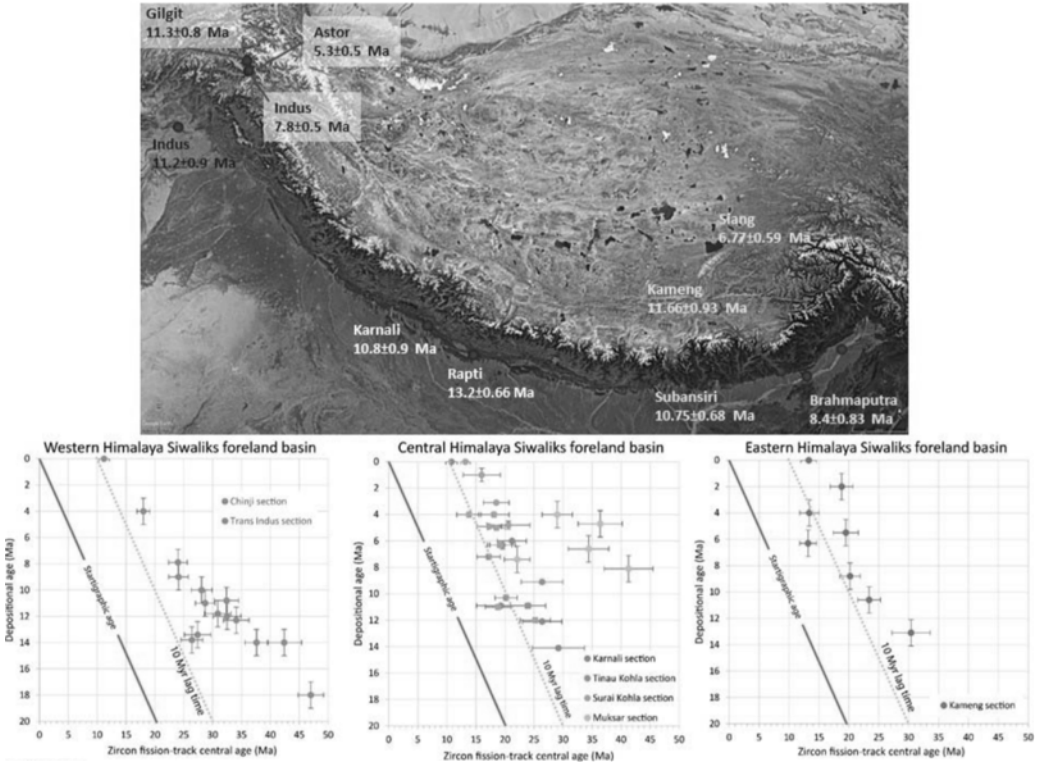

Figure 1.22. *Detrital zircon fission-track central ages of modern river and Siwalik foreland basin sediments of the Western, Central and Eastern Himalaya (data from Cerveny et al. (1988); Bernet et al. (2006); Chirouze et al. (2012, 2013, 2015); Gemignani et al. (2018)). For a color version of this figure, see www.iste.co.uk/jolivet/fission.zip*

1.6.3. *Thermal histories of sedimentary basins*

The thermal annealing of fission tracks in detrital apatite and zircon causes the loss of source area exhumation and sediment provenance information but provides valuable information on the thermal history of active and inverted clastic sedimentary basins. As detrital apatites and zircons may have been derived from rocks of exhumed apatite or zircon fission-track PAZs (e.g. Figure 1.19), we must pay careful attention to the track lengths histograms as shown in Figure 1.13. The question is, have the detrital apatites or zircons acquired partially annealed tracks during burial in the sedimentary basin, or do they show an inherited partial annealing signal? To answer this question, the lag-time trends of central, minimum or peak ages provide valuable constraints (Figure 1.17(B)).

As soon as the minimum or central ages become significantly younger than the age of deposition, we are probably confronted with partial annealing due to burial heating or heating related to magmatic activity in the basin. In addition, we need to obtain independent information on the thermal history from vitrinite reflectance or RockEval analyses of organic matter, diagenetic information on cementation, fluid inclusions and/or illite crystallinity. Particularly apatite fission-track analysis has been widely applied in hydrocarbon exploration, as the peak of oil maturation occurs at temperatures of full annealing of fission-tracks in apatites of average chemical composition as mentioned above (Figure 1.5). See Schneider and Issler (2019) for a recent summary on the application of fission-track analysis to hydrocarbon exploration.

Apatite fission-track data from stratigraphic sections of inverted basins may provide the timing of basin inversion. For example, the timing of basin inversion at around 2 Ma of the Siwaliks foreland basin that is exposed today between the Main boundary thrust and the Main frontal thrust on the southern edge of the Himalaya was documented by thermal history modeling of apatite fission-track ages and track length data (van der Beek et al. 2006) (Figure 1.23). As always, any geological interpretation has to be carefully considered in the light of additional independent geological information and the geodynamic framework of the study area.

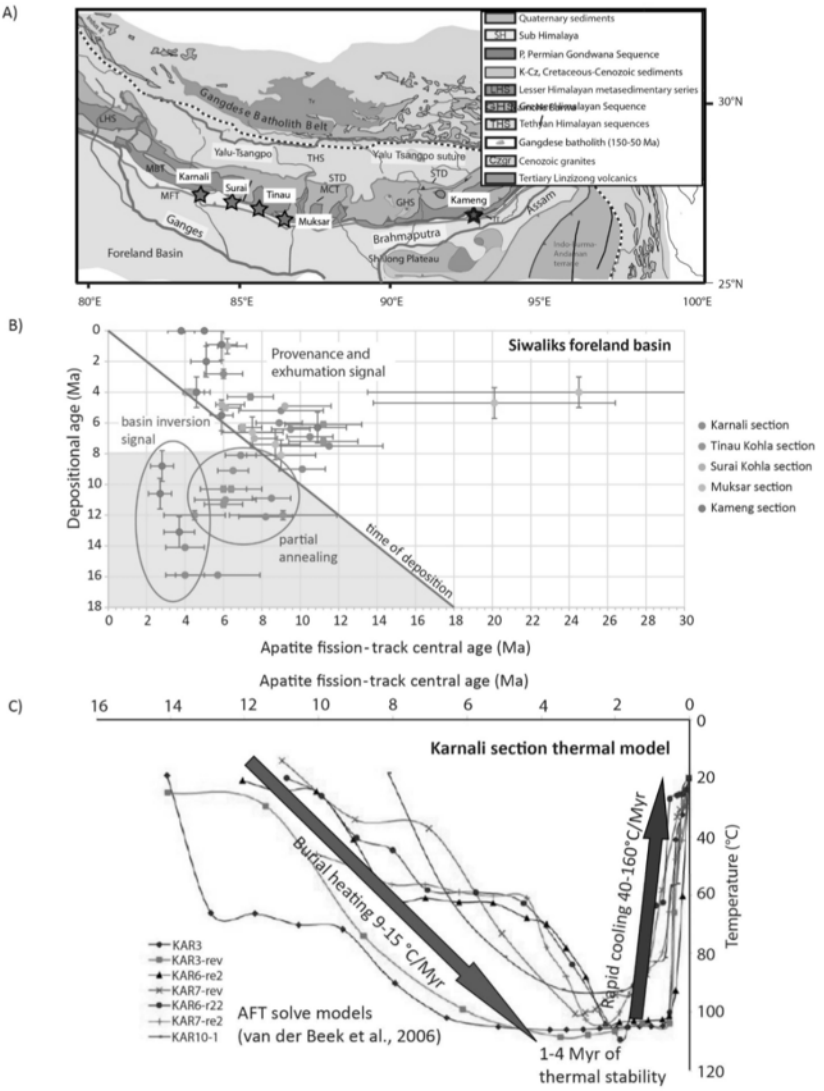

Figure 1.23. *(A) Simplified geological map of the Central and Eastern Himalaya and the Siwaliks foreland basin. Red stars show the locations of the Karnali, Surai, Tinau, Muksar and Kameng sections. Map modified from Chirouze et al. (2013). (B) Apatite fission-track central ages versus depositional age of the Karnali, Surai, Tinau, Muksar and Kameng sections. Data from van der Beek et al. (2006) and Chirouze et al. (2012, 2013). (C) Thermal history models of some of the Karnali section apatite fission-track samples (van der Beek et al. 2006). For a color version of this figure, see www.iste.co.uk/jolivet/fission.zip*

1.7. Concluding remarks

Fission-track dating of detrital apatite and zircon is a powerful tool that can provide valuable information for solving a range of geological problems. Used by itself or in combination with other techniques, we have to keep in mind where the strengths and weaknesses of this approach lie in order to derive a reasonable interpretation of the data and select the appropriate combination of techniques. This chapter is a mere introduction to detrital fission-track thermochronology. A series of books and review articles are recommended here for the interested reader to learn more about fission-track thermochronology and its applications. Some of the fundamental information on fission-track dating are available in the books by Fleischer et al. (1975); and Wagner and Van den haute (1992); and the review paper by Gallagher et al. (1998), now representing classic fission-track literature. The books by Braun et al. (2006) on quantitative thermochronology, and by Reiners and Ehlers (2005), as well as the review paper by Reiners and Brandon (2006), provide a broad introduction to low-temperature thermochronology and its applications, whereas the book by Bernet and Spiegel (2004) is on different aspects of detrital thermochronology. For those who want to better understand the underlying statistics of fission-track dating, particularly for the EDM, the book by Galbraith (2005) is recommended. Finally, a reccent compilation of knowledge on fission-track dating can be found in the book by Malusà and Fitzgerald (2019), with many chapters on the basics of fission-track dating and its applications to geological problems.

1.8. References

van Andel, T.H. (1955). *Sediments of the Rhône Delta. I. Grain Size and Microfauna. II. Sources and Deposition of Heavy Minerals*. De Gruyter Mouton, Amsterdam.

Armstrong, P.A. (2005). Thermochronometers in sedimentary basins. Low-temperature thermochronology: Techniques, interpretations, and applications. *Reviews in Mineralogy and Geochemistry*, 58, 499–525.

Ault, A.K., Gautheron, C., King, G.E. (2019). Innovations in (U–Th)/He, fission track, and trapped charge thermochronometry with applications to earthquakes, weathering, surface-mantle connections, and the growth and decay of mountains. *Tectonics*, 38(11), 3705–3739. doi: 10.1029/2018TC005312.

Barbarand, J., Carter, A., Wood, I., Hurford, T. (2003). Compositional and structural control of fission-track annealing in apatite. *Chemical Geology*, 198, 107–137.

van der Beek, P., Robert, X., Mugnier, J.-L., Bernet, M., Huyghe, P., Labrin, E. (2006) Late Miocene – Recent denudation of the central Himalaya and recycling in the foreland basin assessed by detrital apatite fission-track thermochronology of Siwalik sediments, Nepal. *Basin Research*, 18, 413–434.

Bermúdez, M.A., van der Beek, P., Bernet, M. (2013). Strong tectonic and weak climatic control on exhumation rates in the Venezuelan Andes. *Lithosphere*, 5, 3–16. doi: 10.1130/L212.1.

Bermúdez, M.A., Hoorn, C., Bernet, M., Carrillo, E., van der Beek, P.A., Garver, J.I., Mora, J.L., Mehrkian, K. (2017). The detrital record of Late-Miocene to Pliocene surface uplift and exhumation of the Venezuelan Andes in the Maracaibo and Barinas foreland basins. *Basin Research*, 29, 370–395. doi: 10.1111/bre.12154.

Bernet, M. (2019). Exhumation studies of mountain belts based on detrital fission-track analysis on sand and sandstones. In *Fission-track Thermochronology and Its Application to Geology*, Malusà, M. and Fitzgerald, P. (eds). Springer, Cham.

Bernet, M. and Garver, J.I. (2005). Fission-track analysis of detrital zircon. In *Low-temperature Thermochronology: Techniques, Interpretations, and Applications*, Reiners, P.W. and Ehlers, T.A. (eds). Mineralogical Society of America, Chantilly.

Bernet, M. and Spiegel, C. (eds) (2004). *Detrital Thermochronology – Provenance Analysis, Exhumation and Landscape Evolution of Mountain Belts*. Geological Society of America (Special Publication), Boulder.

Bernet, M., Zattin, M., Garver, J.I., Brandon, M.T., Vance, J.A. (2001). Steady-state exhumation of the European Alps. *Geology*, 29, 35–38.

Bernet, M., Brandon, M.T., Garver, J.I., Molitor, B. (2004a). Fundamentals of detrital zircon fission-track analysis for provenance and exhumation studies. In *Detrital Thermochronology – Provenance Analysis, Exhumation and Landscape Evolution of Mountain Belts*, Bernet, M. and Spiegel, C. (eds). Geological Society of America (Special Publication), Boulder.

Bernet, M., Brandon, M.T., Garver, J.I., Molitor, B. (2004b). Downstream changes of Alpine zircon fission-track ages in the Rhône and Rhine rivers. *Journal of Sedimentary Research*, 74, 82–94.

Bernet, M., van der Beek, P., Pik, R., Huyghe, P., Mugnier, J.-L., Labrin, E., Szulc, A. (2006). Miocene to recent exhumation of the central Himalaya determined from combined detrital zircon fission-track and U/Pb analysis of Siwalik sediments, western Nepal. *Basin Research*, 18, 393–412.

Bernet, M., Brandon, M.T., Garver, J.I., Balestrieri, M.L., Ventura, B., Zattin, M. (2009). Exhuming the Alps through time: Clues from detrital zircon fission-track ages. *Basin Research*, 21, 781–798.

Bernet, M., Urueña, C., Amaya, S., Peña, M.L. (2016). New thermo- and geochronological constraints on the Pliocene-Pleistocene eruption history of the Paipa-Iza volcanic complex, Eastern Cordillera, Colombia. *Journal of Volcanology and Geothermal Research*, 327, 299–309.

Brandon, M.T. (1992). Decomposition of fission-track grain-age distributions. *American Journal of Science*, 292, 535–564.

Brandon, M.T. and Vance, J.A. (1992). Tectonic evolution of the Cenozoic Olympic subduction complex, Washington State, as deduced from fission-track ages for detrital zircons. *American Journal of Science*, 292, 565–565.

Brandon, M.T., Roden-Tice, M.K., Garver, J.I. (1998). Late Cenozoic exhumation of the Cascadia accretionary wedge in the Olympic Mountains, northwest Washington State. *Geological Society of America Bulletin*, 110, 985–1009.

Braun, J. (2003). Pecube: A new finite-element code to solve the 3D heat transport equation including the effects of a time-varying, finite amplitude surface topography. *Computers & Geosciences*, 29, 787–794.

Braun, J. (2016). Strong imprint of past orogenic events on the thermochronological record. *Tectonophysics*, 683, 325–332.

Braun, J., van der Beek, P., Batt, G. (2006). *Quantitative Thermochronology: Numerical Methods for the Interpretation of Thermochronological Data*. Cambridge University Press, Cambridge. doi: 10.1017/CBO9780511616433.

Braun, J.A., van der Beek, P., Valla, P., Robert, X., Herman, F., Glotzbach, C., Pedersen, V., Simon-Labric, T., Prigent, C. (2012). Quantifying rates of landscape evolution and tectonic processes by thermochronology and numerical modeling of crustal heat transport using PECUBE. *Tectonophysics*, 524–525, 1–28.

Briggs, N.D., Naeser, C.W., McCulloh, T.H. (1981). Thermal history of sedimentary basins by fission-track dating. *Nuclear Tracks*, 5(1–2), 235–237.

Caballero, V., Parra, M., Mora, A., Lopez, C., Rojar, L.E., Quintero, I. (2013). Factors controlling selective abandonment and reactivation in thick-skin orogens: A case study in the Magdalena Valley, Colombia. In *Thick-Skin-Dominated Orogens: From Initial Inversion to Full Accretion*, Nemcok, M., Mora, A.R., Cosgrove, J.W. (eds). Geological Society (Special Publications), London. doi: 10.1144/SP377.4.

Carlson, W.D., Donelick, R.A., Ketcham, R.A. (1999). Variability of apatite fission-track annealing kinetics: I. Experimental results. *American Mineralogist*, 84, 1213–1223.

Carrapa, B., DeCelles, P.G., Reiners, P.W., Gehrels, G.E., Sudo, M. (2009). Apatite triple dating and white mica $^{40}Ar/^{39}Ar$ thermochronology of syntectonic detritus in the Central Andes: A multiphase tectonothermal history. *Geology*, 37, 407–410.

Carter, A. (1999). Present status and future avenues of source region discrimination and characterization using fission track analysis. *Sedimentary Geology*, 124, 31–45.

Carter, A. (2007). Heavy minerals and detrital fission-track thermochronology. *Dev. Sedimentol.*, 58, 851–868.

Carter, A. (2019). Thermochronology on sand and sandstones for stratigraphic and provenance studies. In *Fission-Track Thermochronology and Its Application to Geology*, Malusà, M.G. and Fitzgerald, P.G. (eds). Springer, Cham.

Carter, A. and Bristow, C.S. (2000). Detrital zircon geochronology: Enhancing the quality of sedimentary source information through improved methodology and combined U-Pb and fission-track techniques. *Basin Research*, 12, 47–57.

Carter, A. and Bristow, C.S. (2003). Linking hinterland evolution and continental basin sedimentation by using detrital zircon thermochronology: A study of the Khorat Plateau Basin, eastern Thailand. *Basin Research*, 15, 271–285.

Carter, A. and Foster, G. (2009). Improving constraints on apatite provenance: Nd measurement on FT dated grains. In *Thermochronological Methods*: *From Paleotemperature Constraints to Landscape Evolution Models*, Lisker, F., Ventura, B., Glasmacher, U.A. (eds). Geological Society (Special Publications), London, 1–16.

Carter, A. and Moss, S.J. (1999). Combined detrital-zircon fission-track and U-Pb dating: A new approach to understanding hinterland evolution. *Geology*, 27, 235–238.

Cerveny, P.F., Naeser, N.D., Zeitler, P.K., Naeser, C.W., Johnson, N.M. (1988). History of uplift and relief of the Himalaya during the past 18 million years: Evidence from fission-track ages of detrital zircons from sandstones of the Siwalik Group. In *New Perspectives in Basin Analysis*, Kleinspehn, K. and Paola, C. (eds). Springer-Verlag, New York.

Chirouze, F., Bernet, M., Huyghe, P., Erens, V., Dupont-Nivet, G., Senebier, F. (2012). Detrital thermochronology and sediment petrology of the middle Siwaliks along the Muksar Khola section in eastern Nepal. *Journal of Asian Earth Sciences*, 44, 117–135.

Chirouze, F., Huyghe, P., van der Beek, P., Chauvel, C., Chakraborty, T., Dupont-Nivet, G., Bernet, M. (2013). Tectonics, exhumation and drainage evolution of the Eastern Himalaya since 13 Ma from detrital geochemistry and thermochronology, Kameng River Section, Arunachal Pradesh. *Geological Society of America Bulletin*, 125, 523–538.

Chirouze, F., Huyghe, P., Chauvel, C., van der Beek, P., Bernet, M., Mugnier, J.L. (2015). Stable drainage pattern and variable exhumation in the western Himalaya since the Middle Miocene. *Journal of Geology*, 123, 1–20.

Dodson, M.H. (1973). Closure temperature in cooling geochronological and petrological systems. *Contribution to Mineralogy and Petrology*, 40, 259–274.

Donelick, R.A., Ketcham, R.A., Carlson, W.D. (1999). Variability of apatite fission-track annealing kinetics: II. Crystallographic orientation effects. *American Mineralogist*, 84, 1224–1234.

Donelick, R.A., O'Sullivan, P.B., Ketcham, R.A. (2005). Apatite fission-track analysis. In *Low-temperature Thermochronology: Techniques, Interpretations, and Applications*, Reiners, P.W. and Ehlers, T.A. (eds). Mineralogical Society of America, Chantilly.

Dow, W.G. (1977). Kerogen studies and geological interpretations. *Journal of Geochemical Exploration*, 7, 79–99.

Ehlers, T.A., Chaudhri, T., Kumar, S., Fuller, C.S., Willett, S.D., Ketcham, R.A., Brandon, M.T., Belton, D.X., Kohn, B.P., Gleadow, A.J.W. et al. (2005). Computational tools for low-temperature thermochronometer interpretation. In *Low-temperature Thermochronology: Techniques, Interpretations, and Applications*, Reiners, P.W. and Ehlers, T.A. (eds). Mineralogical Society of America, Chantilly.

Enkelmann, E., Zeitler, P.K., Pavlis, T.L., Garver, J.I., Ridgway, K.D. (2009a). Intense localized rock uplift and erosion in the St Elias orogen of Alaska. *Nature Geoscience*, 2, 360–363. doi: 10.1038/NGEO502.

Enkelmann, E., Garver, J.I., Pavlis, T.L. (2009b). Rapid exhumation of ice-covered rocks of the Chugach–St. Elias orogen, Southeast Alaska. *Geology*, 36, 915–918.

Farley, K.A. (2002). (U-Th)/He dating: Techniques, calibrations, and applications. *Noble Gas Geochemistry and Cosmochemistry*, 47, 819–843.

Fitzgerald, P.G., Malusà, M.G., Muñoz, J.A. (2019). Detrital thermochronology using conglomerates and cobbles. In *Fission-track Thermochronology and Its Application to Geology*, Malusà, M. and Fitzgerald, P. (eds). Springer, Cham.

Fleischer, R.L. and Price, P.B. (1964). Techniques for geological dating of minerals by chemical etching of fission fragment tracks. *Ceochimica et Cosmochimica Acta*, 28, 755–760.

Fleischer, R.L., Price, P.B., Symes, E.M., Miller, S.D. (1964). Fission-track ages and track annealing behaviour of some micas. *Science*, 143, 349–351.

Fleischer, R.L., Price, B.B., Walker, R.M. (1975). *Nuclear Tracks in Solids – Principles and Applications*. University of California Press, Berkeley.

Foster, G.L. and Carter, A. (2007). Insights into the patterns and locations of erosion in the Himalaya – A combined fission-track and in situ Sm–Nd isotopic study of detrital apatite. *Earth and Planetary Science Letters*, 257, 407–418.

Galbraith, R.F. (2005). *Statistics for Fission Track Analysis*. Chapman and Hall, Boca Raton.

Galbraith, R.F. and Laslett, G.M. (1993). Statistical models for mixed fission-track ages. *Nuclear Tracks and Radiation Measurements*, 21, 459–470.

Gallagher, K. (2012). Transdimensional inverse thermal history modeling for quantitative thermochronology. *Journal of Geophysical Research*, 117, B02408.

Gallagher, K., Brown, R., Johnson, C. (1998). Fission track analysis and its application to geological problems. *Annual Review of Earth and Planetary Science*, 26, 519–572.

Garver, J.I. and Brandon, M.T. (1994a). Erosional denudation of the British Columbia Coast Ranges as determined from fission-track ages of detrital zircon from the Tofino basin, Olympic Peninsula, Washington. *Geological Society of America Bulletin*, 106, 1398–1412.

Garver, J.I. and Brandon, M.T. (1994b). Fission-track ages of detrital zircons from Cretaceous strata, southern British Columbia: Implications for the Baja BC hypothesis. *Tectonics*, 13, 401–420.

Garver, J.I. and Kamp, P.J.J. (2002). Integration of zircon color and zircon fission-track zonation patterns in orogenic belts: Application to the Southern Alps, New Zealand. *Tectonophysics*, 349, 203–219.

Garver, J.I., Brandon, M.T., Roden-Tice, M., Kamp, P.J.J. (1999). Exhumation history of orogenic highlands determined by detrital fission-track thermochronology. In *Exhumation Processes: Normal Faulting, Ductile Flow and Erosion*, Ring, U., Brandon, M.T., Lister, G.S., Willett, S.D. (eds). Geological Society of London (Special Publication), London.

Gemignani, L., van der Beek, P.A., Braun, J., Najman, Y., Bernet, M., Garzanti, E., Wijbrans, J.R. (2018). Downstream evolution of the thermochronologic age signal in the Brahmaputra catchment (eastern Himalaya): Implications for the detrital record of erosion. *Earth and Planetary Science Letters*, 499, 48–61.

Gérard, B., Robert, X., Grujic, D., Gautheron, C., Audin, L., Bernet, M., Balvay, M. (2022). Zircon (U-Th)/He closure temperature lower than apatite thermochronometric systems: Reconciliation of a paradox. *Minerals*, 12, 145. doi: 10.3390/min12020145.

Glotzbach, C., Bernet, M., van der Beek, P. (2011). Detrital thermochronology records changing source areas and steady exhumation in the Western and Central European Alps. *Geology*, 39, 239–242.

Green, P.F. and Durani, S.A. (1977). Annealin studies of tracks in crystals. *Nuclear Tracks*, 1, 33–39.

Green, P.F., Duddy, I.R., Gleadow, A.J.W., Tingate, P.R., Laslett, G.M. (1986). Thermal annealing of fission tracks in apatite: 1. A quantitative description. *Chemical Geology (Isotope Geoscience Section)*, 59, 237–253.

Guenthner, W.R., Reiners, P.W., Ketcham, R.A., Nasdala, L., Giester, G. (2013). Helium diffusion in natural zircon: Radiation damage, anisotropy, and the interpretation of zircon (U-Th)/He thermochronology. *American Journal of Science*, 313, 145–198.

Guenthner, W.R., Reiners, P.W., Drake, H., Tillberg, M. (2017). Zircon, titanite and apatite (U-Th)/He ages and age-eY correlations from the Fennoscandian Shield, southern Sweden. *Tectonics*, 36, 1254–1274.

Hurford, A.J. (1998). Zeta: The ultimate solution to fission-track analysis calibration or just an interim measure? In *Advances in Fission-Track Geochronology*, Van den haute, P. and de Corte, F. (eds). Kluwer Academic Publishers, Dordrecht.

Hurford, A.J. (2019). A historical perspective on fission-track thermochronology. In *Fission-track Thermochronology and Its Application to Geology*, Malusà, M. and Fitzgerald, P. (eds). Springer, Cham.

Hurford, A.J. and Carter, A. (1991). The role of fission track dating in discrimination of provenance. In *The Role of Fission Track Dating in Discrimination of Provenance*, Morton, A.C., Todd, S.P., Haughton, P.D.W. (eds). Geological Society (Special Publications), London.

Hurford, A.J., Fitch, F.J., Clarke, A. (1984). Resolution of the age structure of the detrital zircon populations of two lower Cretaceous sandstones from the Weald of England by fission track dating. *Geological Magazine*, 121, 269–277.

Huyghe, P., Bernet, M., Galy, A., Naylor, M., Cruz, J., Gyawalie, B.R., Gemignani, L., Mugnier J.L. (2020). Rapid exhumation since at least 13 Ma in the Himalaya recorded by detrital apatite fission-track dating of Bengal fan (IODP Expedition 354) and modern Himalayan river sediments. *Earth and Planetary Science Letters*, 534, 116078. doi: 10.1016/j.epsl.2020.116078

Jourdan, S., Bernet, M., Tricart, P., Hardwick, E., Paquette, J.L., Guillot, S., Dumont, T., Schwartz, S. (2013). Short-lived fast erosional exhumation of the internal Western Alps during the late Early Oligocene: Constraints from geo-thermochronology of pro- and retro-side foreland basin sediments. *Lithosphere*, 5, 211–225.

Ketcham, R.A. (2005). Forward and inverse modeling of low-temperature thermochronometry data. In *Low-temperature Thermochronology: Techniques, Interpretations, and Applications: Reviews in Mineralogy and Geochemistry*, Reiners, P.W. and Ehlers, T.A. (eds). Mineralogical Society of America, Chantilly.

Ketcham, R.A., Donelick, R.A., Carlson, W.D. (1999). Variability of apatite fission-track annealing kinetics. III. Extrapolation to geological time scales. *American Mineralogist*, 84, 1235–1255.

Ketcham, R.A., Carter, A., Donelick, R.A., Barbarand, J., Hurford, A. (2007). Improved modeling of fission-track annealing in apatite. *American Mineralogist*, 92, 799–810.

Ketcham, R.A., Carter, A., Hurford, A.J. (2015). Inter-laboratory comparison of fission track confined length and etch figure measurements in apatite. *American Mineralogist*, 100, 1452–1468.

Ketcham, R.A., van der Beek, P., Barbarand, J., Bernet, M., Gautheron, C. (2018). Reproducibility of thermal history reconstruction from apatite fission-track and (U-Th)/He data. *Geochemistry, Geophysics, Geosystems*, 19, 2411–2436.

Kohn, B., Chung, L., Gleadow, A. (2019). Fission-track analysis: Field collection, sample preparation and data acquisition. In *Fission-track Thermochronology and Its Application to Geology*, Malusà, M. and Fitzgerald, P. (eds). Springer, Cham.

Laslett, G.M., Green, P.F., Duddy, I.R., Gleadow, A.J.W. (1987). Thermal annealing of fission-tracks in apatite, 2. A quantitative analysis. *Chemical Geology (Isotope Geoscience Section)*, 63, 1–13.

Malusà, M.G. (2019). A guide for interpreting complex detrital age patterns in stratigraphic sequences. In *Fission-track Thermochronology and Its Application to Geology*, Malusà, M. and Fitzgerald, P. (eds). Springer, Cham.

Malusà, M.G. and Fitzgerald, P.G. (eds). (2019). Application of thermochronology to geologic problems: Bedrock and detrital approaches. In *Fission-track Thermochronology and Its Application to Geology*. Springer, Cham.

Malusà, M.G. and Fitzgerald, P.G. (2020). The geologic interpretation of the detrital thermochronology record within a stratigraphic framework, with examples from the European Alps, Taiwan and the Himalayas. *Earth Science Reviews*, 201, 103074.

Malusà, M.G. and Garzanti, E. (2019). The sedimentology of detrital thermochronology. In *Fission-track Thermochronology and Its Application to Geology*, Malusà, M. and Fitzgerald, P. (eds). Springer, Cham.

Mark, C., Cogné, N., Chew, D. (2016). Tracking exhumation and drainage divide migration of the Western Alps: A test of the apatite U-Pb thermochronometer as a detrital provenance tool. *Geological Society of America Bulletin*, 128, 143901460.

Montario, M.J. and Garver, J.I. (2009). The thermal evolution of the Grenville terrane revealed through U-Pb and fission-track analysis of detrital zircon from Cambro-Ordovician quartz arenites of the Potsdam and Galway formations. *Journal Geology*, 117, 595–614.

Naeser, C.W. (1981). The fading of fission tracks in the geological environment – Data from deep drill holes. *Nuclear Tracks*, 5(1–2), 248–250.

Naeser, C.W. and Dodge, F.C.W. (1969). Fission track ages of accessory minerals from granitic rocks of the Central Sierra Nevada batholith, California. *Geological Society of America Bulletin*, 80, 2201–2212.

Naeser, N.D., Zeitler, P.K., Naeser, C.W., Cerveny, P.F. (1987). Provenance studies by fission track dating – Etching and counting procedures. *Nuclear Tracks and Radiation Measurements*, 13, 121–126.

Naylor, M., Sinclair, H., Bernet, M., van der Beek, P., Kirstein, L. (2015). Bias in detrital fission track grain-age populations: Implications for reconstructing changing erosion rates. *Earth and Planetary Science Letters*, 422, 94–104.

O'Sullivan, P.B. (1999). Thermochronology, denudation and variations in palaeosurface temperature: A case study from the North Slope foreland basin, Alaska. *Basin Research*, 11, 191–204.

Parra, M., Mora, A., Sobel, E.R., Strecker, M.R., González, R. (2009). Episodic orogenic front migration in the northern Andes: Constraints from low-temperature thermochronology in the Eastern Cordillera, Colombia. *Tectonics*, 28, TC4004.

Parra, M., Mora, A., Lopez, C., Rojas, L.E., Horton, B.K. (2012). Detecting earliest shortening and deformation advance in thrust belt hinterlands: Example from the Colombian Andes. *Geology*, 40, 175–178. doi: 10.1130/G32519.1

Price, P.B. and Walker, R.M. (1962). Observation of fossil particle tracks in natural Micas. *Nature*, 196, 732–734.

Rahn, M.K., Brandon, M.T., Batt, G.E., Garver, J.I. (2004). A zero-damage model for fission-track annealing in zircon. *American Mineralogist*, 89, 473–484.

Rahn, M.K., Wang, H., Dunkl, I. (2019). A natural long-term annealing experiment for the zircon fission-track system in the Songpan-Garzê flysch, China. *Terra Nova*, 1–11. doi: 10.1111/ter.12399.

Reiners, P.W. (2005). Zircon (U-Th)/He analysis. In *Low-temperature Thermochronology: Techniques, Interpretations, and Applications. Reviews in Mineralogy and Geochemistry*, Reiners, P.W. and Ehlers, T.A. (eds). Mineralogical Society of America, Chantilly.

Reiners, P.W. and Brandon, M.T. (2006). Using thermochronology to understand orogenic erosion. *Annual Review of Earth and Planetary Science*, 34, 419–466.

Reiners, P.W. and Ehlers, T.A. (eds). (2005). *Low-temperature Thermochronology: Techniques, Interpretations, and Applications*. Mineralogical Society of America, Chantilly.

Reiners, P.W., Campbell, I.H., Nicolescu, S., Allen, C.M., Hourigan, J.K., Garver, J.I., Mattinson, J.M., Cowan, D.S. (2005). (U-Th)/(He-Pb) double dating of detrital zircons. *American Journal of Science*, 305, 259–311.

Roncancio, J. (2014). Origen de los sedimentos del Cretácico basal (formaciones Yaví y Alpujarra), y su significado tectónico, Cuenca del Valle Superior del Magdalena – Colombia. Master's Thesis (unpublished), Universidad EAFIT, Medellín.

Ruiz, G.M.H., Seward, D., Winkler, W. (2004). Detrital thermochronology – A new perspective on hinterland tectonics, an example from the Andean Amazon Basin, Ecuador. *Basin Research*, 16, 413–430.

Schneider, D.A. and Issler, D.R. (2019). Application of low-temperature thermochronology to hydrocarbon exploration. In *Fission-track Thermochronology and Its Application to Geology*, Malusà, M. and Fitzgerald, P. (eds). Springer, Cham.

Spiegel, C., Kuhlemann, J., Dunkl, I., Frisch, W., von Eynatten, H., Balogh, K. (2000). The erosion history of the Central Alps: Evidence from zircon fission-track data of the foreland basin sediments. *Terra Nova*, 12, 163–170.

Stewart, R.J., Hallet, B., Zeitler, P.K., Malloy, M.A., Allen, C.M., Trippett, D. (2008). Brahmaputra sediment flux dominated by highly localized rapid erosion from the easternmost Himalaya. *Geology*, 36, 711–714.

Tagami, T., Galbraith, R.F., Yamada, R., Laslett, G.M. (1998). Revised annealing kinetics of fission tracks in zircon and geological implications. In *Advances in Fission-track Geochronology*, Van den haute, P. and de Corte, F. (eds). Kluwer, Dordrecht.

Trautwein, B., Dunkl, I., Kuhlemann, J., Frisch, W. (2002). Cretaceous tertiary Rhenodanubian flysch wedge (Eastern Alps): Clues to sediment supply and basin configuration from zircon fission-track data. *Terra Nova*, 13, 382–393.

Urueña-Suarez, C.L., Peña-Urueña, M.L., Muñoz-Rocha, J.A., Rayo-Rocha, L.d.P., Villamizar-Escalante, N., Amaya-Ferreira, S., Ibanez-Mejia, M., Bernet, M. (2019). Zircon U–Pb and fission–track dating applied to resolving sediment provenance in modern rivers draining the Eastern and Central Cordilleras, Colombia. In *The Geology of Colombia*, volume 3, Gomez Tapias, J. and Mateus-Zabala, D. (eds). Servicio Geologico Colombiano, Bogota.

Vermeesch, P. (2004). How many grains are needed for a provenance study? *Earth and Planetary Science Letters*, 224, 441–451.

Vermeesch, P. (2009). RadialPlotter: A Java application for fission track, luminescence and other radial plots. *Radiation Measurements*, 44, 409–410.

Vermeesch, P. (2019). Statistics for fission-track thermochronology. In *Fission-track Thermochronology and Its Application to Geology*, Malusà, M. and Fitzgerald, P. (eds). Springer, Cham.

Wagner, G.A. (1968). Fission-track dating of apatite. *Earth and Planetary Science Letters*, 4, 411–415.

Wagner, G.A. and Van den haute, P. (1992). *Fission-Track Dating*. Kluwer Academic Publishers, Dordrecht.

Willett, S.D. and Brandon, M.T. (2013). Some analytical methods for converting thermochronometric age to erosion rate. *Geochemistry, Geophysics, Geosystems*, 14, 209–222.

Yamada, R., Tagami, T., Nishimura, S., Ito, H. (1995). Annealing kinetics of fission tracks in zircon: An experimental study. *Chemical Geology (Isotope Geoscience Section)*, 104, 251–259.

Yamada, R., Murakami, M., Tagami, T. (2007). Statistical modeling of annealing kinetics of fission tracks in zircon; reassessment of laboratory experiments. *Chemical Geology*, 236, 75–91.